Universidade de Aveiro Departamento de Electrónica, Telecomunicações e Informática,
2016

Sérgio Magalhães Dias

Análise do desempenho de OFDM-PON nas proximas gerações de redes opticas de acesso

Performance Analysis of OFDM-PON in Next Generation Optical Access Networks

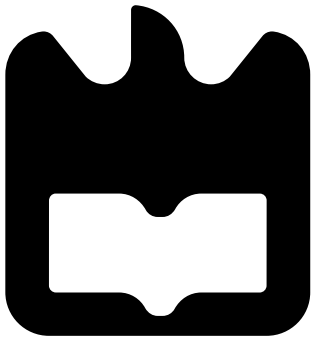

Sérgio
Magalhães Dias

Análise do desempenho de OFDM-PON nas proximas gerações de redes opticas de acesso

Performance Analysis of OFDM-PON in Next Generation Optical Access Networks

Dissertação apresentada à Universidade de Aveiro para cumprimento dos requesitos necessários à obtenção do grau de Mestre em Engenharia Eletrónica e Telecomunicações, realizada sob orientação científica do Dr. António Luís Jesus Teixeira, Professor Associado com Agregação, pertencente ao Departamento de Eletrónica, Telecomunicações e Informática da Universidade de Aveiro e ao Instituto de Telecomunicações e sob Co-orientação científica de Ali Shahpari do Instituto de Telecomunicações.

o júri / the jury

presidente / president

Professor Doutor Armando Humberto Moreira Nolasco Pinto
Professor Associado da Universidade de Aveiro

vogais / examiners committee

Professor Doutor António Luís Jesus Teixeira
Professor Associado c/ Agregação (orientador)

Professor Doutor Pedro Renato Tavares de Pinho
Professor Adjunto do Instituto Superior de Engenharia de Lisboa

agradecimentos / acknowledgements

Assim acabam os melhores 5 anos na Universidade de Aveiro, com alturas boas e outras menos boas, estas ultrapassadas sempre com os melhores ao meu lado.

Começo por agradecer a toda a minha família que são basicamente os pilares de toda a minha força para seguir em frente e de nunca ter desistido nos momentos mais difíceis. Aos meus pais pelo investimento e a confiança no meu sucesso, e às minhas irmãs e cunhados pelo apoio durante todo este meu percurso académico.

Muitos foram os amigos que me deram força e apoio nesta caminhada, não podendo referir todos eles, mas cada um destes sabe a importância que teve e o quão agradecido estou por toda a ajuda.

Alguns agradecimentos têm tambem de ser feitos a pessoas que foram cruciais para o desenvolvimento e conclusão desta dissertação. Agradeço ao Professor António Teixeira, Orientador, e ao Professor Mário Lima, colaborador, por toda a disponibilidade e ajuda prestada nos momentos de mais dificuldade, e claro, agradecer ao Ali Shahpari, porque tudo o que sei da prática é devido a ele e devido á sua grande paciência que teve comigo em laboratório. Um agradecimento muito especial também é feito ao mestre do processamento digital de sinal, Eng. Dr. Ricardo M. Ferreira, que me ajudou em bastantes problemas relacionados com o meu sinal em MATLAB.

Agradeço assim por último todos aqueles que partilharam comigo a sala de ótica no Instituto de Telecomunicações, o André Barros, fiel companheiro de laboratório, Carla Rodrigues e Tiago Morgado, os mestres da ótica integrada e ao André Aranha, amigo de grandes gargalhadas e futura promessa da Seleção Portuguesa de Futebol.

Depois de todos os agradecimentos, peço também desculpa a todas estas pessoas pelas chatices que lhes dei.

Concluindo, há que manter a estrada mesmo na curva apertada.

Resumo

As redes óticas têm vindo a evoluir por forma a conseguir acompanhar a crescente necessidade de largura de banda. Orthogonal frequency division multiplexing (OFDM) tem sido utilizado com sucesso em numerosos standards digitais para uma ampla gama de aplicações, tais como a transmissão de áudio/vídeo digital e sistemas de comunicação wireline/wireless. A atractividade do OFDM resulta de uma boa eficiência espectral e uma redução da interferência entre símbolos. Neste trabalho tentou-se combinar as qualidades do OFDM com as características únicas de uma Passive Optical Network (PON) por forma a compreender se este cenário é ou não viável e em que condições o poder ser.

No transmissor ótico, o OFDM é gerado através de processamento digital de sinal (DSP) usando a transformada inversa de Fourier (IFFT). Este sinal processado é convertido para o domínio RF e depois endereçado a um mecanismo de modulação ótica que o transforma num sinal ótico pronto para a transmissão. Vários moduladores vão ser testados, as suas características serão descritas e um estudo acerca do seu impacto no sistema será efectuado. No receptor, o campo ótico do sinal é reconstruído por deteção direta e em seguida, é aplicado o processamento digital de sinal inverso para assim os dados originais serem recuperados. A qualidade do sinal será discutida através de métodos de avaliação, onde as aplicações dos vários sinais são comparadas de modo a caracterizar o desempenho do sistema.

Assim inicialmente, foi apresentada e demonstrada uma arquitetura de transmissão OFDM-PON nos links upstream usando um modulador externo de Mach-Zehnder (MZM), com agregação de tráfego por multiplexação de banda ortogonal e formatos de modulação avançados. Como alternativa, utilizou-se um método de modulação de baixo custo, baseado em Reflective Semi-conductor Amplifier (RSOA), com um sinal OFDM de 625 Mbit/s. Ambas as experiências usaram o mesmo setup de recepção para comparação. O RSOA apresenta uma largura de banda eléctrica limitada e por isso não permite muito maior largura de banda ou ritmo de transmissão.

O OFDM-PON demonstra que é uma solução alternativa eficiente para as redes óticas de acesso baseadas em aplicações rádio sobre fibra. Este trabalho visa a validação de uma arquitetura OFDM-PON com um bit rate de 10 Gbit/s usando formatos de modulação avançados como QPSK e 16-QAM, de modo a conseguir tirar mais partido das capacidades da fibra.

Abstract

Optical networks have been improving in order to follow the growth bandwidth demand. Orthogonal frequency division multiplexing (OFDM) has been successfully employed into numerous digital standards for broad-range of applications such as digital audio/video broadcasting and wireline/wireless communication systems. OFDM is an attractive solution since it has good spectral efficiency and an efficient symbol interference reduction. In this work, it was studied the combination of the qualities from OFDM with the unique characteristics of a Passive Optical Network (PON) in order to understand if this scenario is feasible and which conditions it can be.

In the transmitter side, the OFDM is generated by digital signal processing (DSP) using inverse fast Fourier transformation (IFFT). The processed signal is converted into the RF domain and then addressed to an optical modulation mechanism that transform it in an optical signal for the transmission. Different modulators will be tested and their characteristics described. In the receiver side, the optical signal is reconstructed by direct detection and then inverse digital signal processing is applied to retrieve the original data. The signal quality will be discussed through evaluation methods, where the signals applications are compared in order to characterize the system performance.

Thus, an OFDM-PON transmission architecture was presented and demonstrated in upstream links using an external modulator Mach-Zehnder (MZM), with traffic aggregation by orthogonal band multiplexing and advanced modulation formats. As an alternative, a low cost modulation method based on the Reflective Semi-conductor Amplifier (RSOA) was used with an OFDM signal of 625 Mbit/s. The reception setup was used for both experiments in order to compare their results. RSOA has limited electrical bandwidth and therefore does not allow higher bandwidth or transmission rate.

The OFDM-PON demonstrates to be an efficient alternative solution for optical access networks based on radio over fiber applications. This work aims the validation of an OFDM-PON architecture with a bit rate of 10 Gbit/s using advanced modulation formats such as QPSK and 16-QAM, in order to take full advantage of fiber capabilities.

Contents

List of Figures

List of Tables

Acronyms

ADC	Analog to Digital Converter
APD	Avalanche Photodiode
AWG	Arrayed Waveguide Grating
B2B	Back to Back
BER	Bit Error Rate
CP	Cyclic Prefix
CW	Continuous Wave
DAC	Digital to Analog Converter
DC	Direct Current
DFT	Discrete Fourier Transform
DSB	Double Side Band
DSP	Digital Signal Processing
EDFA	Erbium Doped Fiber Amplifiers
E/O	Electrical to Optical
ER	Extinction Ratio
EVM	Error Vector Magnitude
FDM	Frequency Division Multiplexing
FFT	Fast Fourier Transform
FTTx	Fiber to the Building/Cabinet/Cell/Curb/Home/Office/Premises
GPON	Gigabit-Capable Passive Optical Network
ICI	Inter Carrier Interference
IDFT	Inverse Discrete Fourier Transform
IFFT	Inverse Fast Fourier Transform

ISI	Intersymbol Interference
ISO	Isolator
MZM	Mach Zehnder Modulator
NG-PON	Next Generation Passive Optical Network
NRZ	Non Return to Zero
O/E	Optical to Electrical
OFDM	Orthogonal Frequency Division Multiplexing
OFDMA	Orthogonal Frequency Division Multiplexing Access
ONU	Optical Network Unit
OLT	Optical Line Termination
OSA	Optical Spectrum Analyzer
OSC	Oscilloscope
P2P	Point-to-point
PM	Power Meter
PON	Passive Optical Network
QAM	Quadrature Amplitude Modulation
QP	Quadrature Point
QPSK	Quadrature Phase Shift Keying
RF	Radio Frequency
RSOA	Reflective Semiconductor Optical Amplifier
Rx	Receiver
SNR	Signal to Noise Ratio
SSMF	Standard Single Mode Fiber
TDM	Time Division Multiplexing
TDMA	Time Division Multiplexing Access
TTA	10 Gbit/s Tunable Transmitter Assembly
TWDM	Time Wavelength Multiplexed
Tx	Transmitter
VOA	Variable Optical Attenuator

VPI	Virtual Photonics Incorporated
WDM	Wavelenth Division Multiplexing
XG-PON	10 Gigabit-Capable Passive Optical Network

Chapter 1

Introduction

1.1 Context and Motivation

The continuous increase in the bandwidth demand led to the capacity saturation of electrical-based systems. Thus, optical communication comes to operate at higher data rates in backbone and metropolitan networks. An electrical system operating at a data rate of 200 Mbit/s needs to be regenerated every kilometer during the transmission. Optical systems operate at gigabit data rates and the regeneration of the optical signal is only needed over hundreds of kilometers [1].

One of the biggest concerns is the compatibility of an old optical network with future optical networks. These days in most of the countries, the optical network are based on point to point (P2P) connections, where human intervention is needed. Thus, the modern optical networks are evolving in order to be highly adaptive and reconfigurable. The use of these reconfigurable optical networks minimizes the requirement of human intervention and consequently minimizes associated costs.

The first standards passive optical networks (PON) to appear ensuring a bigger data rate was the Ethernet passive optical network (EPON) and Gigabit-Capable passive optical network (GPON), but soon they will not be able to satisfy the clients needs. Thus, several others standards PON was created to ensure higher data rate as the Next Generation passive optical network (NG-PON) [2]. Two types of NG-PON were created, the NG-PON1 that uses a 10 Gigabit-Capable Passive Optical Network (XG-PON) technology combined with GPON by a Wavelength Division Multiplexing (WDM) system, and the NG-PON2 which at the beginning had several proposed technologies, such as WDM-PON, Ultra Dense Wavelength Division Multiplexing (UDWDM) -PON [3], Orthogonal frequency division multiplexing (OFDM)-PON and Time Wavelength Division Multiplex (TWDM)-PON. Among these, TWDM-PON technology was considered to be the NG-PON2 solution, because it was less disruptive and featured less risk and best price than the others solutions.

The aim of this work is to show that the OFDM-PON is another powerful technology in order to deliver a higher bandwidth to a huge number of applications to ensure a higher transmissions speed. This technology is a combination of modulation and multiplexing that shares the bandwidth among individual modulated data sources.

OFDM signal has many advantages, such as the efficient spectrum, due to the subcarriers overlapped, elimination of the Inter-symbol interference (ISI), due the use of a cyclic prefix (CP), and computational efficiency, by using the Inverse Fast Fourier transform (IFFT) to perform the modulation and the Fast Fourier transform (FFT) to perform the demodulation.

1.2 Objectives

The main objective of this dissertation is to analyse and demonstrate that the OFDM-PON network is and attractive candidate for future broadband optical access networks. This dissertation was based on the following main objectives:

- Simulation and experimental analysis of OFDM-PON using direct detection.
- To study bidirectional OFDM-PON system using an RSOA in upstream links.
- To identify and classify different m-QAM mapped in each Orthogonal Frequency Division Multiplexing (OFDM) subcarrier and their performance for direct detection.
- OFDM-PON test system over SSMF.

1.3 Document structure

- **Chapter 2: OFDM and OFDM-PON architectures**
  This chapter starts with a overview of the available PON till the present and the associated technologies. After the PON overview, it will be explained what is the OFDM and how it can be generated electrically. Once the signal is generated, it will be further explained how the electrical signal can be transmitted through the optical channel.
- **Chapter 3: Simulation**
  The aim of this chapter is the simulation of the OFDM setup. With the help of the Virtual Photonics Incorporated (VPI), that allows building very complex simulation scenarios of any optical transmission designs, the simulation will be performed and associated results will be presented.
- **Chapter 4: Practical Experiment**
  This chapter presents the laboratory results of two external modulation setup. The first one using a Mach Zehnder Modulator (MZM) and the other using and a Reflective Semiconductor Optical Amplifier (RSOA), both with the same propose - perform the electrical to optical (E/O) conversion.
- **Chapter 5: Conclusion and Future Work**
  In this last chapter, final conclusions of the performed work are discussed and some future research suggestions are proposed.

1.4 Contributions

The main contributions were:

- Demonstration that OFDM-PON is also a good technology for future broadband optical access networks, by testing it under this scenario and over two different modulator technologies.
- Study and implementation of related off-line DSP algorithm at the transmitter to generate the signal and at the receiver to recover the signal.

Chapter 2

OFDM and OFDM PON architectures

In this chapter, it will be discussed some PON infrastructures that can perform an optical communication over a Standard Single Mode Fiber (SSMF). PON have three main parts which allow optical communication. These parts consist of an optical line termination (OLT), located at the central office that provides the interface between the central office and the core network, the optical network unit (ONU), located at the client that provides the interface between the access network and the customer, and the optical distribution network (ODN) providing a physical channel for optical communication between the OLT and ONU over fiber cables, optical connectors and splitters [4].

2.1 Competing Technologies

2.1.1 TDM-PON

To avoid collisions in the upstream transmission, a communication protocol was created to assign a time slot to each client, in order to allow only one ONU transmission at a time. With this protocol comes a new passive optical network named Time Division Multiplexing (TDM)-PON.

In TDM-PON, the OLT is connected to multiple ONUs via 1:N passive optical power splitter near to the client. Each splitter output connects to a subscriber through individual SSMF. The central office at the OLT transmits the traffic in downstream direction, while the ONU transmits the traffic in upstream direction. The end client can be a home, an office or elsewhere. Therefore, it comes up the FTTx concept, where the x is a specific end client. TDM-PON is an architecture that employs a point to multi-point (P2MP) scheme and uses low-cost components for optical networks. One of the biggest concerns of the TDM-PON is its range that is between 10 and 20 km, and there is plenty research performed in order to increase the covered area, and thus increase the number of subscribers. Figure 2.1 illustrates the architecture of a TDM-PON [5].

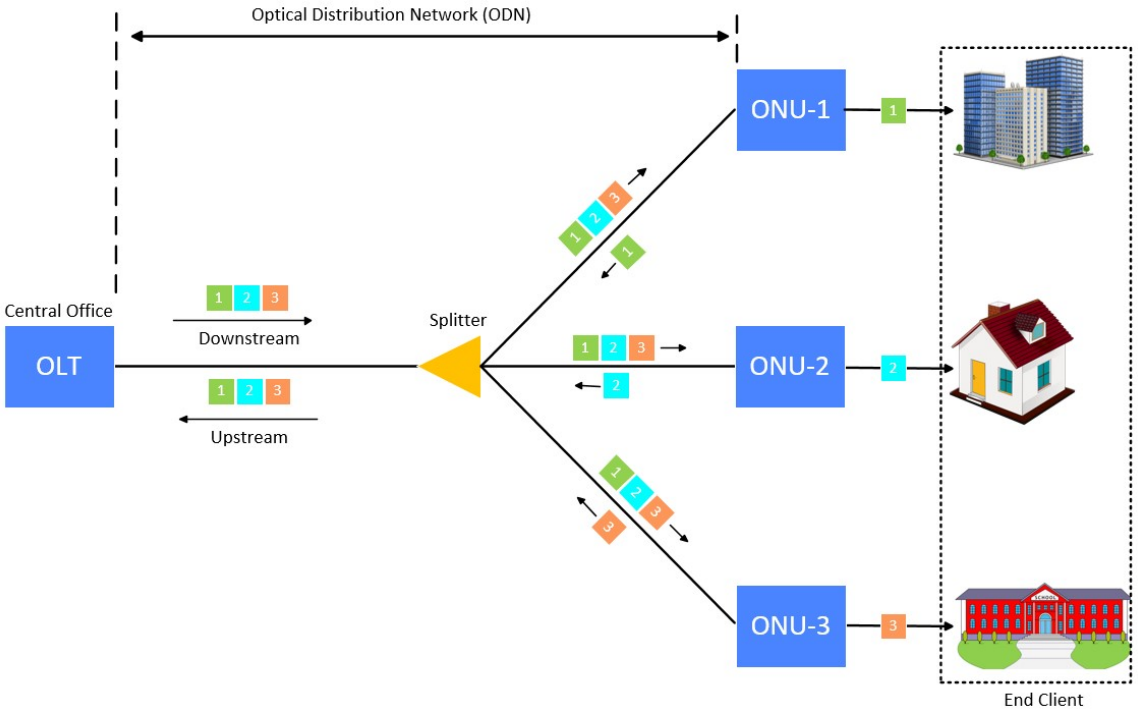

Figure 2.1: TDM PON architecture.

At the OLT side, the signals are sent in time slots to different ONUs each with a frame header that is the ONU identification. The downstream signal is sent through a 1:N passive optical power splitter which sends the signal to all ONUs with the power N times smaller. After the splitter, each ONU reads the frame header in order to obtain the respective slot. In the upstream direction, each ONU transmits in burst-mode due to the fact that all the ONUs want to transmit over the same SSMF [5].

2.1.2 WDM-PON

As clients bandwidth demands continue increasing, it becomes difficult for the TDM-PON to satisfy the bandwidth client requirement. Thus, as the bandwidth demands increase, a new PON has to be created in order to support the bandwidth requirement from each client, so an innovate concept for access network is created, the WDM-PON. Using WDM-PONs, each client gets a much higher bandwidth than the TDM-PONs can offer, because transmitters at the OLT and ONU sides can use multiple wavelengths over a physical P2P fiber infrastructure. However, the upgrade from the current TDM-PON to the WDM-PON has some disadvantages in a cost-effective, flexible and scalable way. Thus, it becomes a strong topic for intense research [5].

Although WDM-PON has been used successfully in long-haul networks, but is quite expensive for access networks. Attending that in long-haul networks the core network cost is shared by multiple clients (millions), while in access networks are shared only for a few (hundreds) clients. Figure 2.2 illustrates the network architecture of WDM-PON [5].

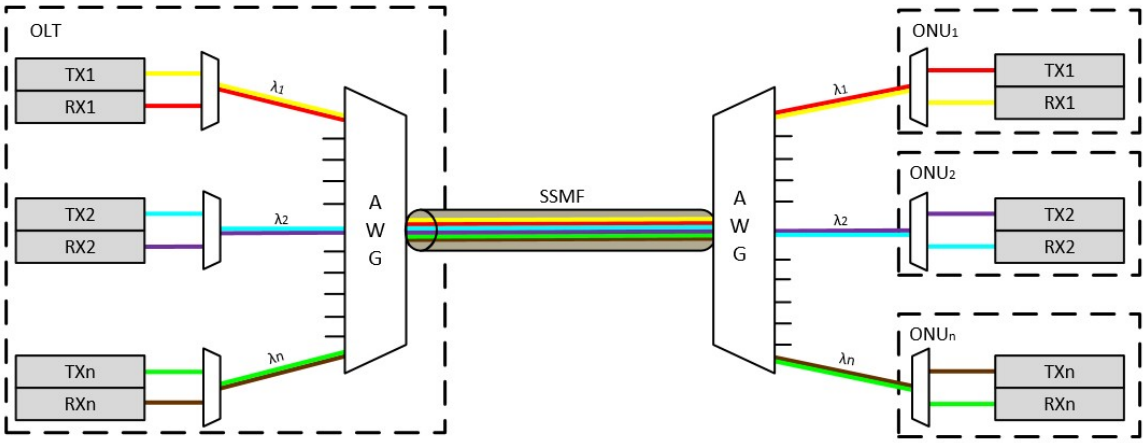

Figure 2.2: WDM PON architecture.

In figure 2.2, it is possible to observe on the left central offices at the OLT, and on the right side the end client at the ONU. Both of them have several transmitters and receivers. Each transmitter-receiver pair at the OLT and ONU side works with a specific wavelength that connects to a port of the arrayed waveguide grating (AWG), that is used as multiplexer/demultiplexer. The AWG at the right side that connects multiple ONUs subscribers, acts like a single PON that has been splitted into multiple PONs. A SSMF is the bridge between both AWGs, the OLT AWG and the ONU AWG in the distribution network. Each transmitter-receiver pair has a passive splitter that connects the transmitted signal and the received signal. The transmitter needs to be set to a specific wavelength [5].

All the transmitters and receivers at the ONU side have to be colorless, it means, wavelength independent, in order to reduce the number of the ONUs to provide more than one client. In other way, if the transmitters and receivers are not wavelength independent, it would be needed a special ONU for each client, generating additional costs. In figure 2.2, all the transmitters and receivers at the ONU are tunable, and can be set to a desired wavelength [6].

2.1.3 TWDM-PON

This technology was selected in 2012 by the Full Service Access Network (FSAN) to be the solution for the NG-PON2 architecture. In TWDM-PON, a WDM is used to stack four XG-PON1s. XG-PON technology provides 10Gbit/s bit rate in the downstream direction and a 2.5Gbit/s in the upstream direction. Thus, four pairs of wavelengths are used at TWDM-PON in order to provide a 40Gbit/s bit rate in downstream and a 10Gbit/s bit rate in the upstream direction with a split ratio of 1:64. Due to this fact, NG-PON2 will be able to meet the rate requirements [7].

The biggest TWDM-PON wavelength constrain is the coexistence of the previous PONs, and several options that have been created. The first option is to reuse the existing XG-PON wavelength bands, defining a smaller grid inside of these bands. The main idea of the TWDM-PON wavelength is the use of the already developed work over XG-PON1. This option is going to be compatible with GPON and radio frequency (RF) video overlay, but XG-PON1 is blocked. The second option is to make use of the C-band in order to contain the downstream and upstream wavelengths. With this option, it is possible to use an Erbium doped fiber

amplifier (EDFA) to amplify the signal to get longer distances with lower transmission losses. This wavelength plan has coexistence with GPON and XG-PON1 with the RF video overlay channel blocked. The third option is a mixture of the first and second options, where the downstream channel is located at L-plus band and the upstream channel is located at the C-minus band. This wavelength plan has coexistence with GPON and RF video overlay with XG-PON1 channel blocked. This option takes an advantage of the EDFA to amplify the downstream direction and pre-amplify the upstream direction [7]. The fourth and last option is where the NG-PON2 has to be able to coexist between the previous standardized technologies, GPON, XG-PON1 and RF video overlay. This system uses the O,E,S,C and L bands. Figure 2.3 shows an example of a TWDM-PON architecture [8].

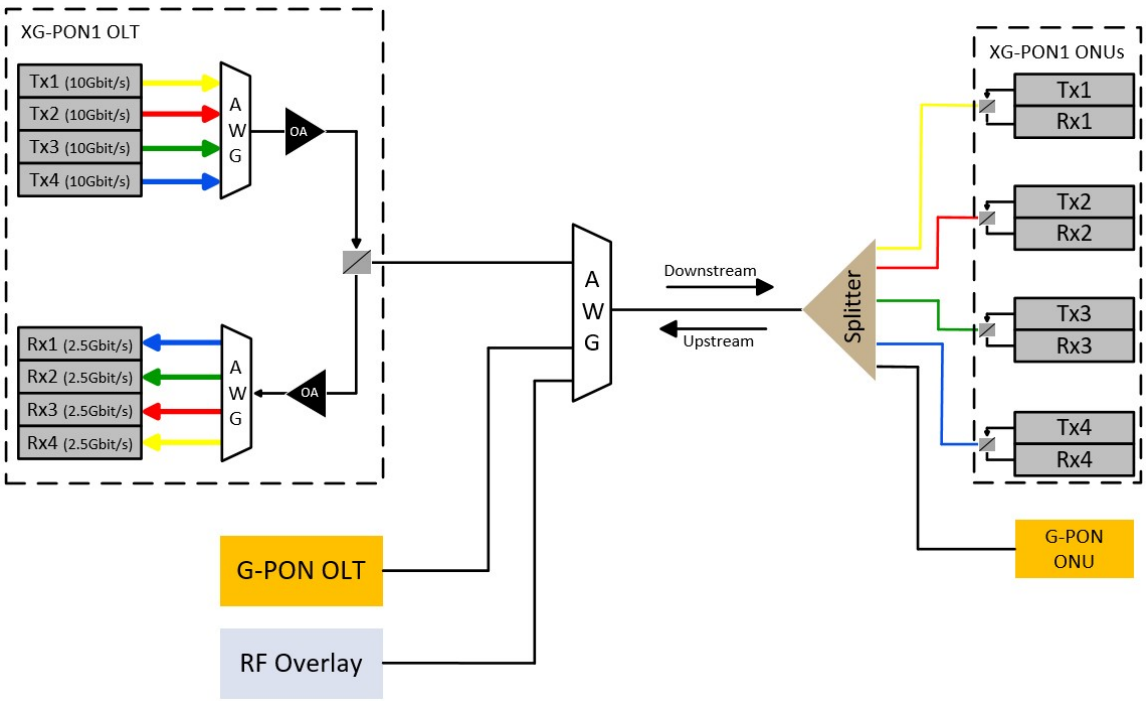

Figure 2.3: TWDM PON architecture.

In figure 2.3, it is possible to observe four XG-PON1s stacked using four pairs of wavelengths. In the central office, each wavelength is multiplexed to obtain the 40 Gbit/s and routed in the downstream direction. After the splitter, each ONU picks the corresponding wavelength (one of the four wavelengths). Because of the coexistence of the current PON, a WDM filter at the central office will be needed. For a simple management the ONU uses colorless transmitters and receivers. The transmitter is tunable to any of the four wavelengths in the upstream direction and the receivers are tunable for any of the four downstream wavelengths. At the OLT side, two essential blocks are used: an optical amplifier to amplify the downstream signal and pre-amplify the upstream signal and two AWGs, the first one to multiplex the different XG-PON1s downstream wavelengths, and the other to demultiplex the upstream wavelengths in order to select the wavelength that was previously selected by the OLT [7].

2.2 OFDM-PON

The OFDM is an excellent solution to be used in PON when applied in long-haul optical communications. The use of the OFDM has many advantages as it will be spoken in section 2.3. To accommodate multiple users, Time Division Multiplexing Access (TDMA), WDM and Orthogonal frequency division multiplexing access (OFDMA) PON systems have been proposed to NG-PON [9]. The downstream transmission of OFDM-PON is a hybrid technique, which combines OFDMA and TDMA. This multiple access technique allows that each OFDM subcarrier can be dynamically splitted to different clients in different time slots in a specific network. Figure 2.4 shows an example of OFDM-PON [10].

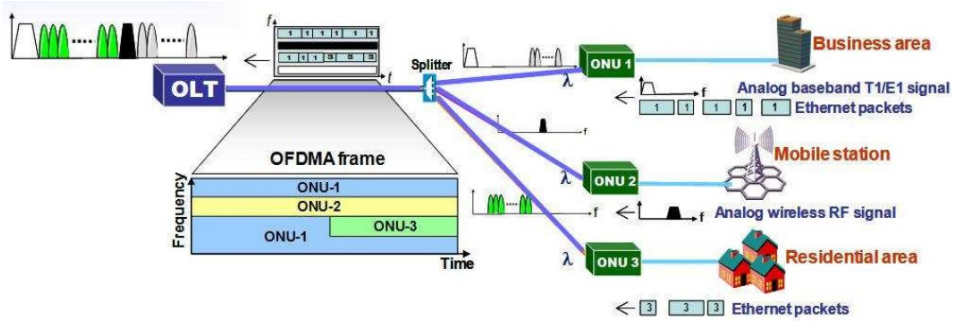

Figure 2.4: OFDMA-PON architecture for delivery of heterogeneous services with single-wavelength upstream transmission [9].

As it is possible to observe in figure 2.4, the bandwidth allocation is performed in time and frequency domains. The OFDMA frame allocated in time and frequency domain is performed by the OLT in the downstream direction, with the resulting time/frequency broadcast to all of the ONUs over non-reserved OFDM subcarriers and pre-configured time slots [9] [10]. Then this OFDMA frame is injected into the SSMF, splitted by a 1:N splitter. At the receiver side, each ONU has a digital signal processing (DSP) in order to recover the associated OFDM subcarriers and/or time slots. In the upstream direction, each ONU modulates the data over the assigned subcarrier set, nulls all remaining ONUs subcarriers, and the OFDM modulation is performed to create a complete frame. This frame passes through a coupler that injects the created ONU frame into the SSMF [10].

2.3 OFDM Basics

OFDM has been study as an interesting technology for optical communications over the last years. The OFDM is a frequency division multiplexing (FDM) special case [11]. FDM is a multicarrier system which has several signals from different information sources. In the transmitter, each signal is modulated with multiple subcarriers within the same single channel (Base band signal multiplied by a sinusoidal carrier f_i), as shown in figure 2.5. The total data rate, that goes to the single channel, is divided between all subcarriers [12]. Each subcarrier is then modulated with the conventional modulation scheme and the receiver has to be able to receive the FDM signal. If the received signal does not have any subcarrier overlapped, with a Band pass filter centered on the frequency f_i, it is possible to obtain the demodulated signal in the output. This system usually needs a guard band interval between each subcarrier, to

prevent overlap of subcarriers.

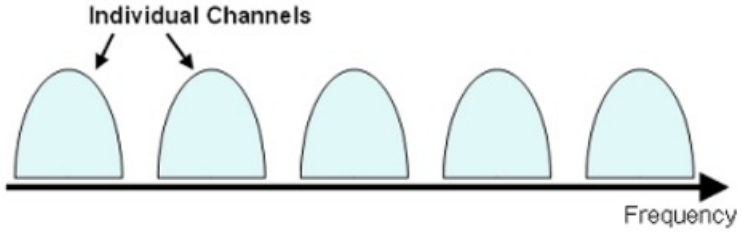

Figure 2.5: FDM channels separated by frequency guard bands [13].

In the other hand, the OFDM, a multi-carrier digital communication, has a single information source, which gives a sequence of information in bits with a high-rate. The guardbands, which was previously presented, are no longer needed, because of the orthogonality propriety. As long the channel is linear, the signal can be recovered without interference, increasing the spectral efficiency.

The transmitted multi-carrier signal s(t) is given by:

$$s(t) = \sum_{i=-\infty}^{+\infty} \sum_{K=1}^{N_{sc}} c_{k,i} \cdot e^{j2\pi f_k t} \cdot P(t - iT_s) \tag{2.1}$$

where the N_{sc} is the number of subcarriers, the T_s is the duration of each OFDM symbol, and the $c_{k,i}$ is the ith information OFDM symbol at the kth subcarrier, f_k is the subcarrier frequency and the $P(t)$ is the pulse shaping function [1]. The f_k has to satisfy the orthogonality condition:

$$f_k = k \cdot \frac{1}{T_s} \tag{2.2}$$

where K is the number of subcarriers, and each subcarrier is separated by $\frac{1}{T_s}$ [1]. The amplitude spectrum of the OFDM signal, is given by a $sinc(\pi f t)$, where all frequencies f_k are multiple of $\frac{1}{T_s}$, as show in figure 2.6.

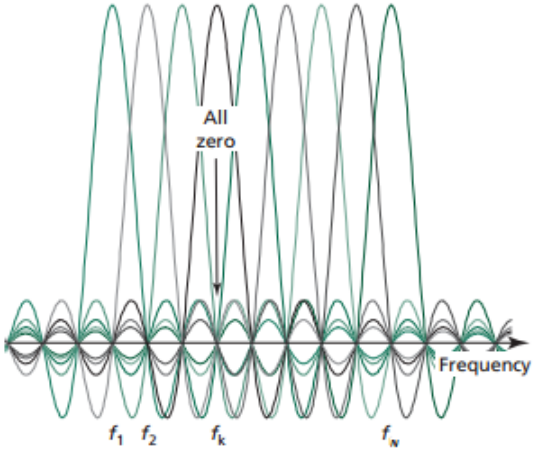

Figure 2.6: OFDM signal spectrum [14].

In figure 2.6, it is possible to conclude that the OFDM spectrum is an overlapping of sinc functions, where each one represents a subcarrier. As seen before, the orthogonality is achieved if the subcarrier is centered in f_k and separated from the neighbor by $\frac{1}{T_s}$, this is an important path for the receiver to recover all the subcarriers without Inter-carrier interference (ICI). In single carrier systems, the symbol duration T_s is given by the reciprocal baud rate $\frac{1}{R}$ and in a multi carrier system is given by $\frac{N}{R}$, where the N is the subcarrier's number [14].

2.4 Electrical OFDM

Creating the OFDM signal has to be done in several stages, as shown in the figure 2.7.

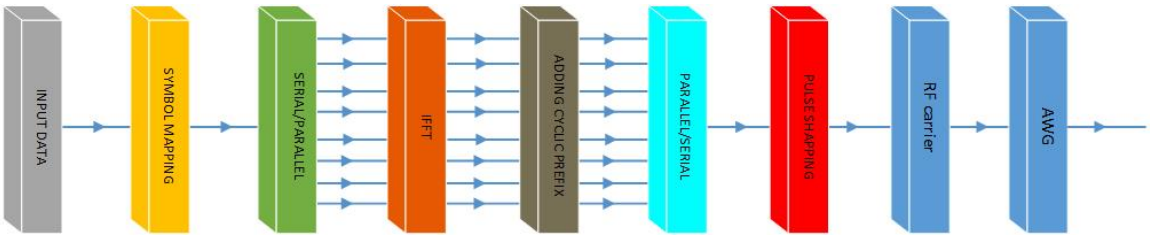

Figure 2.7: Electrical OFDM signal generation.

2.4.1 Mapping and Demapping

After the first stage, where a random bit sequence was generated, comes the second stage, where the bit sequence is mapped in mode to have a certain number of symbols per subcarrier. To perform that, it is used a complex modulation format such as M-Quadrature Amplitude Modulation (QAM) or Quadrature Phase Shift Keying (QPSK). For example, the QPSK modulation uses two by two bits from the input serial data, to create each of the 4 possible complex values symbols, as show in the figure 2.8. In case of selecting a higher order format the system is able to carry more bits of information per symbol.

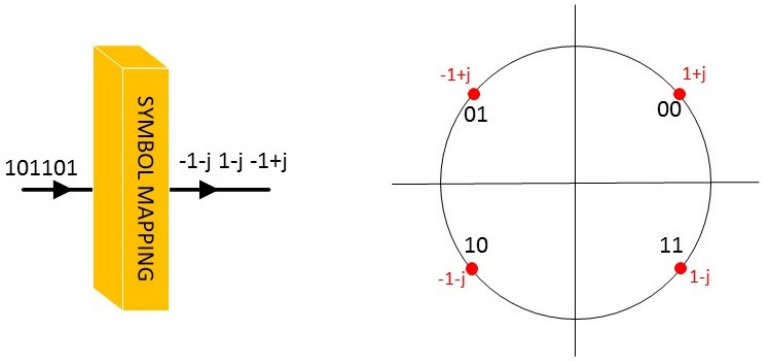

Figure 2.8: QPSK mapping.

At the receiver side, each symbol coming from the parallel/serial block, represented in the received constellation, will be demapped to obtain the original bit sequence from de transmitter. These symbols changed from complex values to real values, as shown in figure 2.9.

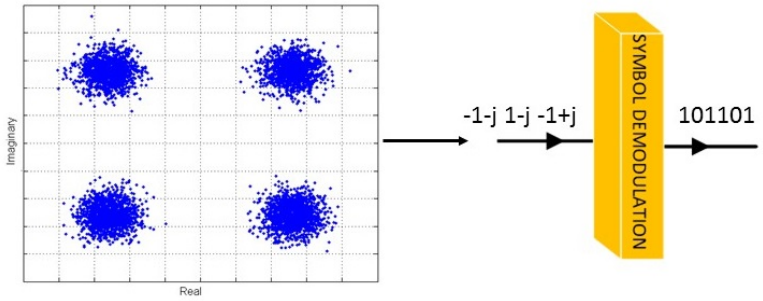

Figure 2.9: QPSK demapping.

However, these symbols arrive with some distortion, because the channel is not ideal. Because of that, a decision limit has to be set to know which constellation point belongs to the distortion point before start demapping the complex values, as will be referred in section 4.1.

2.4.2 Serial to Parallel Conversion and Parallel to Serial Conversion

The subcarriers generation begins in this stage. At the transmitter side, the modulated data is injected into the serial/parallel block, where the data is transformed from a high-speed serial signal into a relative low-speed parallel signal. This low-speed signal corresponds to each output of the serial/parallel block, the so-called sub-carrier, as shown in figure 2.10a.

At the receiver side, each low-speed signal is transformed into a high-speed serial signal. The symbols of each subcarrier are the parallel/serial input, as shown in figure 2.10b. The signal is now ready to be demapped in order to obtain the corresponding bits.

(a) (b)

Figure 2.10: Data conversion (a) shows the serial/parallel block and (b) shows the parallel/serial.

2.4.3 FFT and IFFT

The FFT and IFFT blocks, are the main components in the receiver and transmitter respectively, and these are the essential functions for OFDM to distinguish the single carrier systems [15]. These blocks are widely used in order to change data between the time-domain and frequency-domain. FFT / IFFT blocks are mathematically equivalent versions of Discrete Fourier transform (DFT) and a Inverse Discrete Fourier transform (IDFT) of the received and transmitted OFDM signal, but more efficient to implement [12].

However, to create an OFDM signal with a large number of subcarriers, requires an extremely complex architecture at the transmitter and receiver. In order to observe this phenomenon, in the next equation only one OFDM symbol of the signal s(t) of 2.1 is taken, and s(t) is sampled every interval of $\frac{T_s}{N}$.

$$s(\frac{nT_s}{N}) = \sum_{N-1}^{k=0} c_k e^{j2\pi f_k \frac{nT_s}{N}} = \sum_{N-1}^{k=0} c_k e^{j2\pi \frac{kn}{N}} = \mathcal{F}^{-1}\{c_k\} \tag{2.3}$$

where the $\mathcal{F}$ is the Fourier transform, and n $\in$ [1,N]. At the receiver side, arrives

$$c'_k = \mathcal{F}\{r_m\} \tag{2.4}$$

where r_m is the received signal. The values of the transmitted OFDM signal s(t) is merely a simple N-point IDFT of the information c_k, and the same case can be applied to the receiver, where c'_k is a simple N-point DFT of the received sampled signal [1].

To perform the conversion of frequency-domain data into time-domain data, the IFFT block correlates the frequency-domain input data with its orthogonal basic functions. The IFFT block uses as input the source symbols, that comes of the mapping block, in the frequency-domain that brings the signal into the time-domain, as shown in figure 2.11a.

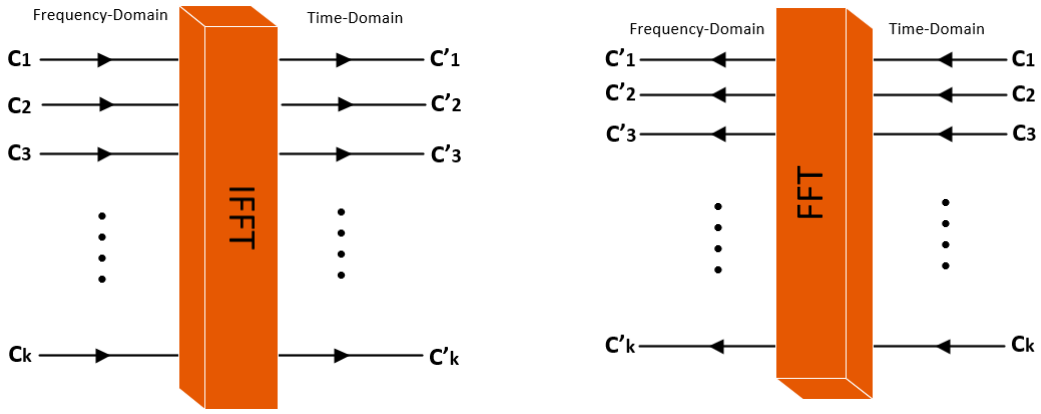

Figure 2.11: Fast Fourier transform (a) IFFT block that transforms the signal into time domain and (b) FFT block that transforms the signal into frequency domain.

After some additional processing parameters, the OFDM signal in the time-domain is transmitted across the channel and arrives to the receiver side. At the receiver side, a FFT block waits for the CP block output, that is in the time-domain, to transform this output in a frequency-domain signal.The FFT outputs will be the same as inputs of the IFFT block at the transmitter side, as shown in figure 2.11b.

2.4.4 Cyclic prefix

At this stage the signal is handled in the time domain. At the transmitter side, the IFFT block outputs are injected into the CP block. Mostly of the OFDM systems use this block to add a CP in the beginning of each OFDM symbol before being transmitted, as shown in figure 2.12a. At the receiver side the CP is also removed as shown in figure 2.12b.

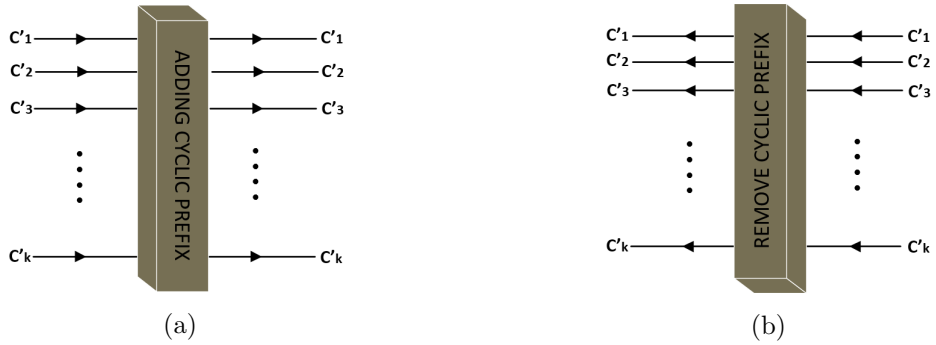

Figure 2.12: Cyclic Prefix (a) Adding the Cyclic prefix at the transmitter and (b) removing the cyclic prefix at the receiver.

On the transmitter side, all the subcarriers are aligned and ready to be transmitted. But when these subcarriers achieve the receptor, some of the OFDM symbols are delayed by a period of time when compared to other subcarriers. This delay is caused by to the channel dispersion, where the slow subcarrier crosses the symbol boundary leading to interference

between neighboring. This interference is known as ISI, where the received OFDM symbol is distorted by other previously transmitted OFDM symbol. Furthermore, because of this delay, the orthogonality is lost, resulting in an inter-carrier interference (ICI) penalty [1] [12]. Thus, some solutions have emerged to prevent this delay. One of these solutions comes with the placement of a blank space to avoid interference of symbols even when it gets delayed. But it is not possible to have blank spaces in signals so, in order to solve this, the end part of the DFT window is copied to the guard interval, located at the beginning of the DFT window, with time shifted forward, the so-called CP [1].

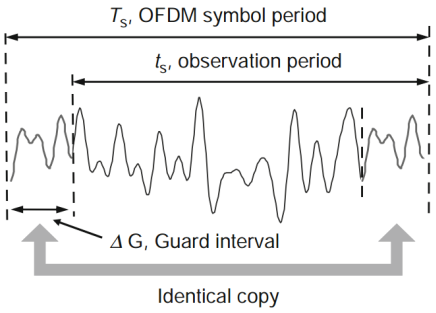

Figure 2.13: The time domain OFDM signal for one complete OFDM symbol [1].

It is shown in figure 2.13 a DFT window of one complete OFDM symbol in the time-domain, with the period of OFDM symbol without the CP (t_s), and the period with the CP (T_s). The CP length should exceed the maximum excess delay of the multi path propagation channel.

2.4.5 Pulse Shapping

One of the biggest problems of the parallel-serial block output signal is the ICI between adjacent sub-carriers, because it affects the performance of this block [16]. Considering this, multiple techniques have been implemented to control the ICI, as the implementation of a pulse-shaping filter, changing the waveform of the signal. With that comes the sixth step, where the signal is filtered by a pulse shaping filter named root raised cosine, where the signal has to satisfy Nyquist ISI criterion [17]. The root raised cosine frequency characteristic is given by the mathematical equation 2.5.

$$X_{rc}(f) = \begin{cases} T & 0 \leq |f| \leq \frac{1-\beta}{2T} \\ \frac{T}{2}\left\{1+\cos\left[\frac{\pi T}{2}\left(|f|-\frac{1-\beta}{2T}\right)\right]\right\} & \frac{1-\beta}{2T} \leq |f| \leq \frac{1+\beta}{2T} \\ 0 & |f| > \frac{1+\beta}{2T} \end{cases} \tag{2.5}$$

The root raised cosine filter is defined by the roll-off factor, β, that controls how sharply the pulse spectrum declines and takes values in range $0 \leq \beta \leq 1$, while T is the symbol interval [18]. Root raised cosine with higher roll-off factor value needs a short symbol interval, but has a disadvantage that is the bigger bandwidth of the spectrum.

2.4.6 RF upconversion

The OFDM signal s(t) is generated at baseband in form of a complex value, and it becomes a real-value signal during the transmission. This complex-to-real-value conversion is performed through a RF modulator with a carrier frequency (f_c). To complete this stage, the signal has to pass through an RF modulator (IQ modulator/demodulator) where the real and imaginary parts of the complex OFDM signal are multiplied by the trigonometric functions cos and sin to obtain the RF signal, as show in equation 2.6.

$$S_{RF}(t) = I\{S(t)\} \cdot \cos(2\pi f_c\, t) - Q\{S(t)\} \cdot \sin(2\pi f_c\, t) \tag{2.6}$$

In equation 2.6, the $S_{RF}(t)$ is now the real-value signal centered at frequency f_c, the $S(t)$ is the complex-value signal after RF modulator in the baseband and the real and imaginary parts corresponding to the in-phase (I) and quadrature (Q) components of the signal $S(t)$ [1].

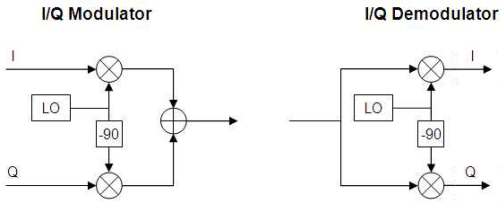

Figure 2.14: Upconversion at the left and downconversion at the right [19].

In figure 2.14 it is shown how an IQ modulator/demodulator looks like. To build these modulators requires a local oscillator with a 90-degree shift in one arm regarding the other, as well as one pair of RF mixers. At the downconversion it is performed the opposite function, returning the OFDM signal to baseband [1].

2.4.7 D/A and A/D conversion

After the parallel-serial block, a digital to analog converter (DAC) is required on the transmitter side, and at the receiver side an analog to digital converter (ADC). The DAC is needed to convert the discrete value of the S_n transmitted to a continuous analog value, $S_n(t)$, and an ADC is needed to convert the continuous analog value received, $r(t)$ signal, to a discrete value, r_m.

2.5 Optical OFDM

In previous section it was shown the generation of the electrical OFDM signal. In order to allow the transmission of this signal through the optical channel, optical modulation is required to change electrical to optical domain at the transmitter, and the opposite at the receiver.

2.5.1 Optical OFDM transmission

The main propose of the transmitter side is to convert electrical signal into an optical signal and then propagate it through the communication channel. In the optical transmitter, the most important component is the optical source, but it is not the only one. Other components like optical modulators are commonly used in combination with semiconductor lasers, and electrical driving current. Two techniques can be used to modulate the optical signal generated by the semiconductor laser, the direct and external modulation [20].

2.5.1.1 Direct Modulation

In direct modulation the light source, a semiconductor, is easily modulated by an electrical signal through its bias current, in RF domain, as input to produce a modulated optical output. This modulation depends on the laser characteristics. In figure 2.15 it is shown a electrical OFDM signal as input, S(t), being modulated over an optical carrier.

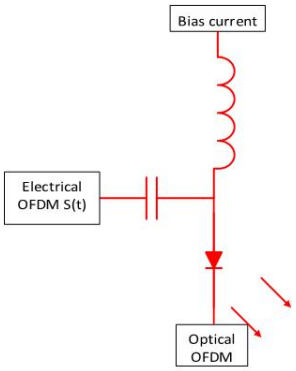

Figure 2.15: Direct modulation.

As the laser turns on and off according to the input current, this causes some problems such as chirp (frequency shift) which increases the signal bandwidth [20]. Because of that, this concept is rarely used to bit rates of 10 Gbit/s or higher. For the laser to obtain gain, the stimulated emission must be dominant, in other words, there has to be a reversal of the population of a state to a higher state.

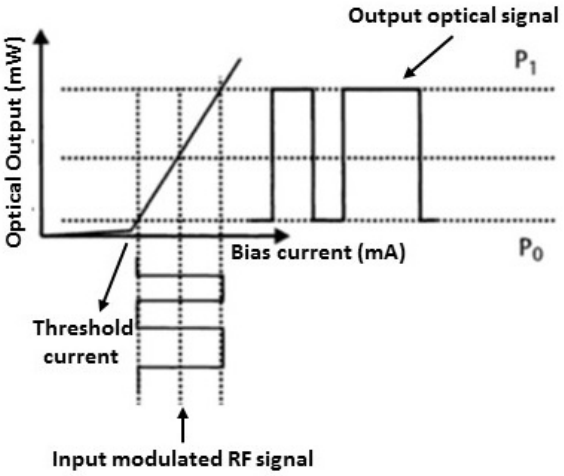

Figure 2.16: L-I curve [21].

The output power is given by the L-I curve, as shown in figure 2.16. It is possible to see that if the bias current is lower than the threshold current the spontaneous emission occurs with a large spectral width and a very small light beam is emitted. If the bias current is higher than the threshold current the stimulated emission occurs, where it is observed an increase of the output power and a decrease of the spectral width. The E/O conversion occurs in the stimulated emission with strong correlation in phase, frequency and direction of radiated photons. When facing the case of bias current higher then the threshold current, if the input signal is too high, the output signal is going to have distortion that limits the output [21].

2.5.1.2 External Modulation

The other technique to modulate the electrical signal, is through an external process after light generation. At bit rates higher or equal to 10 Gbit/s, the external modulation is used, because it produces less chirp than the direct modulation. This external modulator is used to modulate the continuous wave (CW) coming from the semiconductor lasers controlled by a fixed injection current, that creates a constant optical output. This technique is more complex and has more advantages than the direct modulation, like an increase of the bit rate and transmission distance [21]. There are a few options for external modulators to upstream transmission, as MZM and RSOAs.

- **Mach-Zehnder Modulator (MZM) :** The MZM is composed by two arms, each one formed by $LiNbO_3$ material. The input signal is equally split into the two arms, which later will be combined [22]. Both arms have two electrodes, the first one to high-speed ac voltage, the RF signal, and the other for direct current (DC) bias voltage, as shown in figure 2.17.

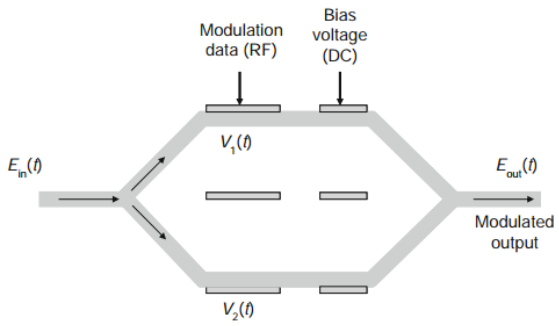

Figure 2.17: Mach-Zehnder modulator [1].

The refractive index of $LiNbO_3$ material changes with DC bias voltage applied in each electrode (upper and lower arms), creating the electro-optic effect. For the DC bias voltage range, the index refractive increases and the speed of light decreases, resulting in a phase shift of the optical signal. The phases in both arms are critical to the desired output. If each arm has an equal refractive index, the output signal is going to be the sum of two light streams in phase, resulting in a high pulse level. If on each arm there is different refractive indexes, the output signal level will be lower. But when the phase difference between the two arms is π, there is a cancellation of the two signal streams and no light is transmitted. In this case, with a certain modulation voltage, an optical bit stream is created [1] [21]. The electrical field at the output, given by the sum of the two signals streams from each arm, is show in the equation 2.7.

$$E_{out}(t) = \frac{E_{in}}{2}\left(e^{j\Delta\phi_1(t)} + e^{j\Delta\phi_2(t)}\right) \tag{2.7}$$

Where the $E_{in}(t)$ is the input electrical field, the $\Delta\phi_i(t)$ is the changes of phase in both arms (i=1,2), due the change of the refractive index n with respective voltage applied in each electrode [23]. The phase changes are given by

$$\Delta_{\phi(i)}(t) = \frac{\pi}{V_\pi}\upsilon_i(t), i = 1, 2 \tag{2.8}$$

where V_π is the differential drive voltage ($\upsilon_1 - \upsilon_2 = V_\pi$), resulting in the phase shift of π between the two arms, and the υ_1 and υ_2 are the voltage values applied in each arm of the MZM. The V_π is the critical value needed to change the output power. Figure 2.18 shows the transfer function of the MZM [23].

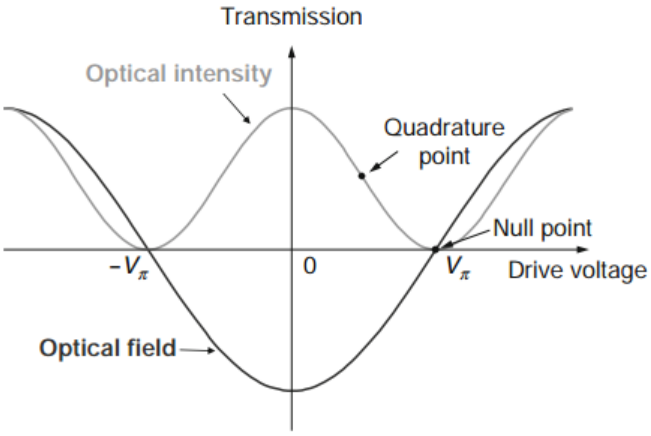

Figure 2.18: MZM transfer function [1].

For a bias voltage of $V_b = (2n-1)\frac{V_\pi}{2}, n = 1, 2, 3...$, the MZM is in the linear response and the intensity modulation is achieved. This point is called the quadrature point (QP). At a bias voltage of $V_b = nV_\pi, n = 1, 2, 3...$, the optical power at the output is the modulated signal, the so-called Null Point (NP) [23]. The result of the MZM output is in double side-band (DSB) optical modulation, being affected with chromatic dispersion, arising RF fading [24].

- **Reflective Semiconductor Optical Amplifiers (RSOAs) :** In order to have a better cost-effective WDM-PONs, a RSOA was implemented, that can simultaneously amplify and modulate the seeded CW. The RSOA has two faces, one with a high reflectivity coating and the other with an ultra low reflectivity coating ($< 10^{-5}$) [25]. The RSOA intensity modulator is composed by InGaAsP semiconductor materials. To amplify and modulate the incoming signal in each ONU a RSOA is used to send the modulated signal through the upstream direction [26]. This intensity modulator has more advantages beside the cost-effectiveness and the fact that can modulate and amplify at the same time, as colorlessness, low power dissipation, compactness and large-scale monolithic integration capability. The analog DSB electrical OFDM signal coming from the DAC is mixed with the DC bias current, in the RSOA, to modulate the CW at 1550 nm, producing the optical OFDM signal ready to pass through the optical channel [27].

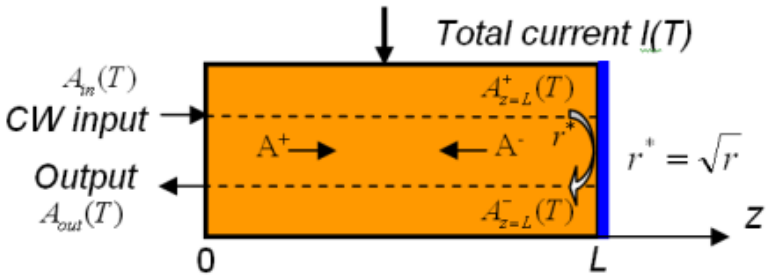

Figure 2.19: RSOA intensity modulator [28].

Figure 2.19 shows the schematic diagram of an RSOA intensity modulator with a cavity of length L and the two faces already introduced, one with high reflectivity coating ($Z = L$) and the other with a ultra low reflectivity coating ($Z = 0$). r is the RSOA reflectivity on $Z = L$. The optical signal is inserted at $Z = 0$ and reflects at the high reflectivity coating, $Z = L$. At $z = 0$, the optical field, $A_{in}(T)$, is added to the RSOA input, and the optical field, $A_{out}(T)$, is the already modulated RSOA output that reflected in the high reflectivity coating ($Z = L$) [28]. The RSOA optical gain,in dB, has to compensate the cavity losses. Gain is given by the equation 2.9.

$$G_{RSOA}(T) = \frac{P_{out}(T)}{P_{in}(T)} = r \cdot exp[2h(T)] \tag{2.9}$$

Where the $P_{out}(T)$ and $P_{in}(T)$ are the powers of the modulated output optical signal and the injected optical signal at $z = 0$. Both powers are in dBm [28].

2.5.2 Optical OFDM receiver

The optical receiver is an essential component of an optical fiber communication system, where the main propose is converting an optical signal into an electrical signal and recover the transmitted data. Optical OFDM is classified in two advanced detection methods, the direct detection system and the coherent detection.

2.5.2.1 Coherent detection

Coherent detection is the most advanced detection method, where the incoming signal, the full electric field, is handled in amplitude and phase. When used coherent detection , the data can be mapped in amplitude and phase, or alternatively in both in-phase (I) and quadrature, which brings a huge flexibility. [29]

At the detection the received signal is combined with a local oscilator in order to recover the transmitted signal. A polarization controller is used by the local oscilator, and this polarization must be set according to the received signal. Thus, with DSP it is possible to recover the amplitude and phase information. [30]

2.5.2.2 Direct detection

The main component to perform the O/E conversion, is a photodetector with photoelectric effect. The principle of the photoelectric effect, consists on photons absorption of the incoming optical signal, and generation of electrical current. It should have a high sensitivity at the operating wavelengths, a large and linear response to the received optical signal, a short response time (time taken by electrons and holes to travel until the electrical contacts) to obtain a good bandwidth, a low noise, independence of environmental changes, a small physical size, a low bias voltage, high reliability and the price of the photodetector has to be low, because it's an important piece in a big optical communication system. The semiconductor photodiodes are the best solution for operate at the receiver [31]. The photocurrent, generated by the photodetector, is proportional to the incident optical power, is given by:

$$I_p = RP_{in} \tag{2.10}$$

Where the I_p is the photocurrent, P_{in} the input optical power, and the R is the responsivity (A/W). The responsivity is used to characterize the performance of the photodetector, measuring the electrical output per optical input, that is related to a fundamental quantity, η, named as quantum efficiency, the ration between the photogenerated electrons and the number of incident photons, given by:

$$\eta = \frac{Electron\ \ Generation\ \ Rate}{Photon\ \ Incidence\ \ Rate} = \frac{I_p/q}{P_{in}/hv} = \frac{hv}{q}R \tag{2.11}$$

Thus from equation 2.11 the responsivity, R, is given by:

$$R = \frac{\eta e}{hf} \tag{2.12}$$

Where the e is the electron charge, h the Planck constant and f the frequency of the optical signal.

Once the optical signal was photodetected, the created electrical signal is downconverted to baseband. Typical photodiodes are the PIN photodiode and the Avalanche Photodiode (APD) [32].

- **PIN:** The PIN photodiode consists in the insertion of a layer of undoped semiconductor material sandwiched between p- and n-type layers. When this layer is under the reverse bias, a depletion layer is created in both sides of the p- and n-type layers, throughout the i-layer, where the absorption takes place [1]. Figure 2.20 shows an example of an structure of a PIN photodiode, where the three layers mentioned.

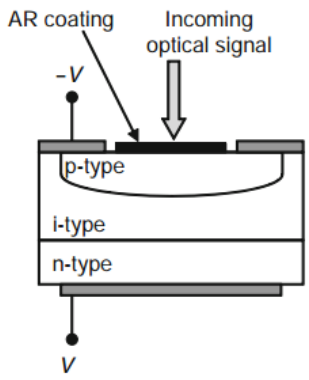

Figure 2.20: Structure of a PIN photodiode [1].

The depth of depletion region can be controlled by changing the i-layer thickness to absorb the maximum number of incident photons. This depletion region, has a very high internal impedance, where a electric field is created . Electron-hole pairs, in the depletion region, are created when the photons arrive at the PIN photodiode input. The electron-hole pairs are separated because of the created electric field, and each part goes in different directions, one part to p- layer and the other to n- layer, in order to obtain the photocurrent proportional to the input optical signal power [32].

- **Avalanche Photodiode (APD):** An APD is just a modified PIN photodiode with a very high reverse bias [1]. The main difference is an additional layer, p-layer, where the holes and electrons can get sufficient kinetic energy to create secondary electron-hole pairs. This process is know as impact ionization. This process leads to an internal gain, where the APD is under a large electric field consequence of a high voltage, as shown in figure 2.21 [31].

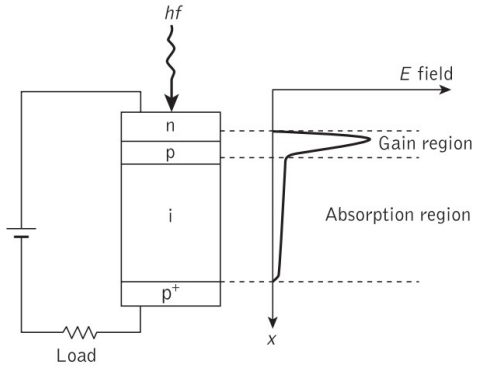

Figure 2.21: Structure of a APD photodiode showing the internal gain region [31].

This electric field in p-layer, located between the i-layer and n^+-layer, is created by a reverse bias. The depletion region continues in the i-layer, with the normal function, creating primary electron-hole pairs due the incoming photons absorption [32]. This generated electron is accelerated ,due the electric field, until collide the target material, where the electron loses some kinetic energy. This collision with the target leads to the already spoken process, the impact ionization, where multiple electrons are created. These new electrons, will be also accelerated until collide the target material. As this process goes on, the electrons and holes created grow exponentially [33]. Because of that, a current amplification is obtained. The internal current gain is given by:

$$M = \frac{I_{APD}}{I_{ph}} \tag{2.13}$$

where the I_{APD} is the total current generated in the APD and I_{ph} is the current created by photon absorption. The responsivity of an APD is related to the quantum efficiency defined by the ability of the incident photons to be absorbed in the depletion region of the photodiode in order to generate electrons. It is defined as:

$$R_{APD} = \frac{\eta q}{hv} \cdot M \tag{2.14}$$

where η is the quantum efficiency, q the electron charge, and hv the Plank's equation that calculates the energy of photons [5].

Chapter 3

Simulation

The software used to perform the simulation based on the OFDM setup was VPI. This is commonly used among Optical Communication research community as it allows building very complex simulation scenarios of any optical transmission designs. VPI offers a vast amount of examples for applications of the software in the demo section. For this work in particular OFDM long-haul demo was used as a starting point for understanding how the VPI works, and then some blocks were added and removed in order to achieve the main goal. This VPI demonstration shows all the concepts explained in the previous chapter, most importantly the E/O effect and the optical to electrical (O/E) effect.

The simulation results that will be presented in this chapter were displayed in other tool, VPI Photonics Analyzer tool. Finally, VPI Transmission Maker was chosen to create and edit the simulation setup.

As it was explained in chapter 2, in order to create an OFDM signal, several stages have to be made. All these stages can be simulated using different blocks in VPI. The OFDM coder and decoder blocks, for instance, can be customized by changing their parameters. Three of these internal parameters are shared between both blocks, Sample Rate, Bit Rate and the number of bits per symbol, thus if any of these parameter is changed, it should be equally changed in both blocks.

3.1 External modulation with MZM using OFDM

In this simulation setup, the OFDM signal is generated at the transmitter side and directly detected at the receiver side after traveling several kilometers over optical fiber. Figure 3.1 shows the simulation scenario for the external modulation with an MZM using an OFDM signal.

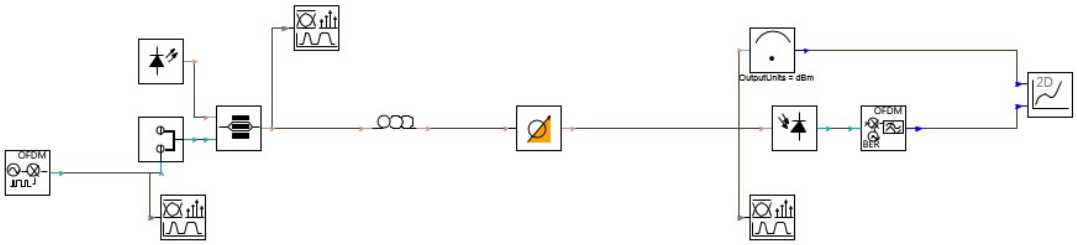

Figure 3.1: External Modulation simulation setup

The OFDM coder, the first block on the left side, has a group of elements in charge of processing the OFDM modulation, explained in section 2.4. To achieve a 10 Gbit/s bit rate requires a 5 GBd symbol rate in QPSK and 2.5 GBd in 16-QAM modulations formats, both using an RF carrier of 5 GHz. As the OFDM signal is upconverted at 5GHz, the signal can now be optically modulated by the MZM together with the laser at CW. After the MZM, the optical OFDM signal is transmitted through a swep control making it cross several kilometers of fiber.

The optical signal is directly detected by a single photodiode that can be a PIN or an APD, resulting in the electrical OFDM signal. This signal goes to the OFDM decoder block which perform the same operations as the transmitter but in a reverse order.

In the transmitter side two signals analyzers were used in order to observe the spectrum before and after the MZM, and in the receiver side another signal analyzer was placed to observe the received spectrum and constellation, and a 2D numerical analyzer in order to obtain the sensitivity of the photodetector. These results will be seen at the simulation results section.

3.1.1 Simulation results

VPI has two types of parameters, the specific ones that belong to a single block, and the global parameters that are constant all blocks in the simulation. Thus, the parameters that can be defined to use in this simulation are shown in table 3.1.

OFDM coder/Decoder	***Value***	***Unit***
Number of subcarriers	8	
Modulation formats	QPSK, 16-QAM	
OFDM symbol rate using QPSK	5	GBd
OFDM symbol Rate using 16-QAM	2.5	GBd
Bit Rate	10	Gbit/s
Carrier Frequency	5	GHz
Bits Per Symbol using QPSK	2	
Bits Per Symbol using 16-QAM	4	
Nyquist Response	Square Root Raised Cosine	

Table 3.1: Simulation Parameters

The parameters of the laser are set to their default values since their effect is not part of this study. The MZM and the optical fiber were also set to their default parameters.

After the optical fiber link, a swep attenuator was applied. This is a useful tool for produce a Bit error rate (BER) versus Received Power plot. This attenuator starts with a received power of 5 dBm and is incremented 1 by 1 until reaching a received power of -30 dBm. The numerical analyzer, at the right side, has inputs for different measured receiver powers and other to receive the BER calculations from the decoder. Comparing it the barrier of 10^{-3} enables viewing the BER versus Received Power plot.

The receiver can be switched between PIN and APD, with a simple parameter in the receiver block. The simulation was performed with two types of modulation formats, QPSK and 16-QAM. The simulation results for both modulation formats are shown in the section 3.1.1.1 and 3.1.1.2.

3.1.1.1 QPSK modulation format

The received optical spectrum, which results from the signal analyzer before the photodiode and after the fiber, is shown in figure 3.2.

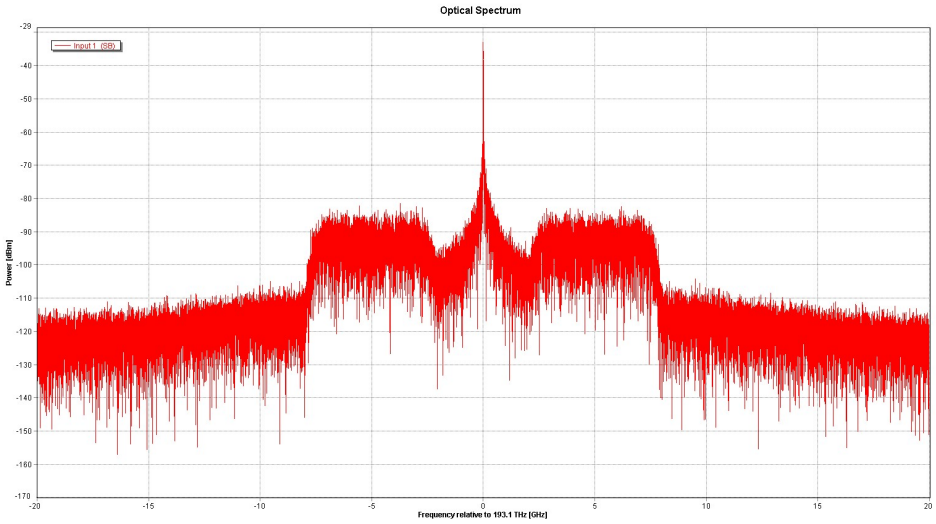

Figure 3.2: QPSK with PIN

As it is possible to observe in figure 3.2, the symbol rate is 5 GBd resulting in a bit rate of 10 Gbit/s as QPSK modulation format has 2 bits per symbol. It is also possible to observe the signal centered at 5 GHz.

Results from the PIN are shown in figure 3.3, and from an APD photodetector in figure 3.4.

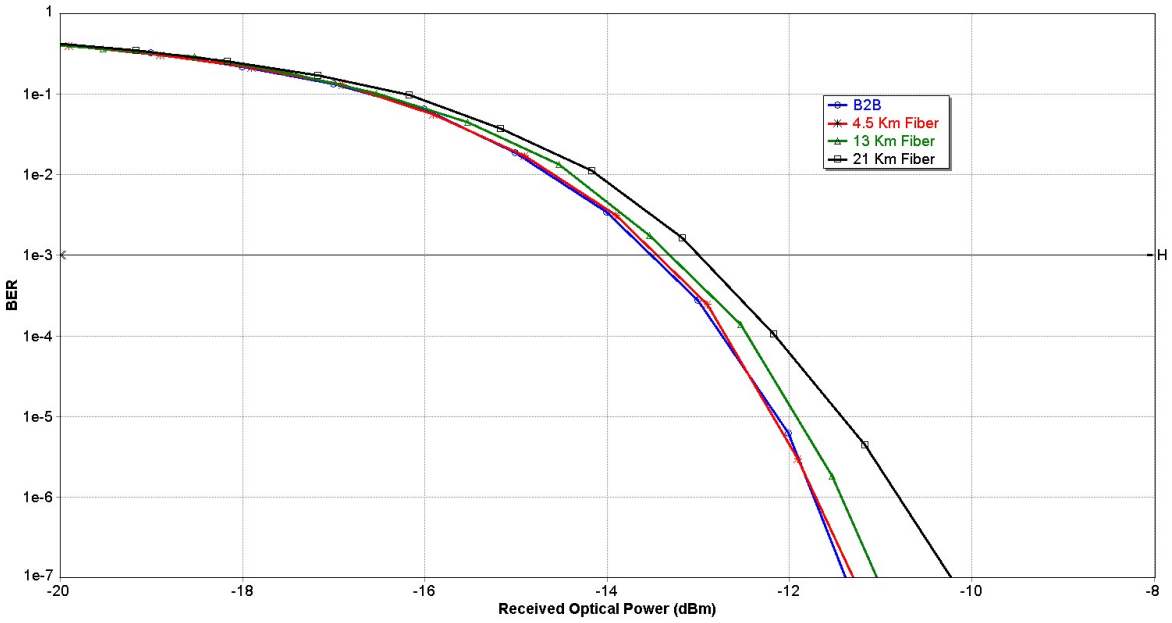

Figure 3.3: QPSK results using a PIN

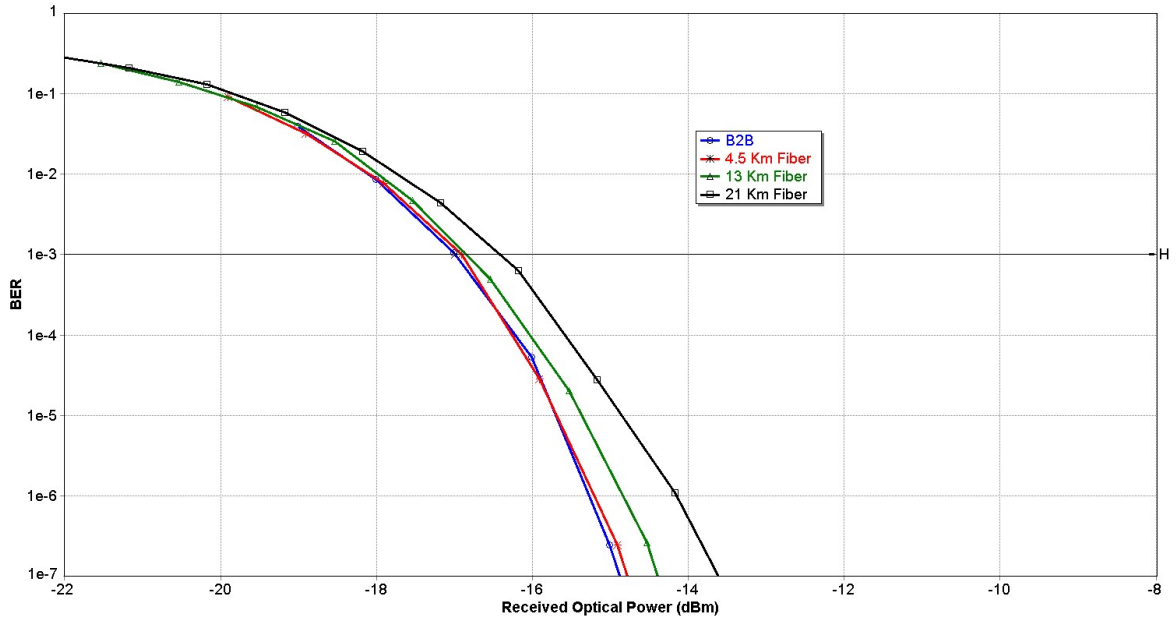

Figure 3.4: QPSK results using a APD

In figure 3.3, it is possible to conclude that the B2B receiver sensitivity is around -13.5 dBm, and in figure 3.4, the B2B the receiver sensitivity is around -17 dBm. The power penalties happen due to the chromatic dispersion, where the optical phase of the signal depends on its wavelength.

3.1.1.2 16QAM modulation format

The received optical spectrum is plotted in figure 3.5, which results from the signal analyzer before the photodiode and after the fiber.

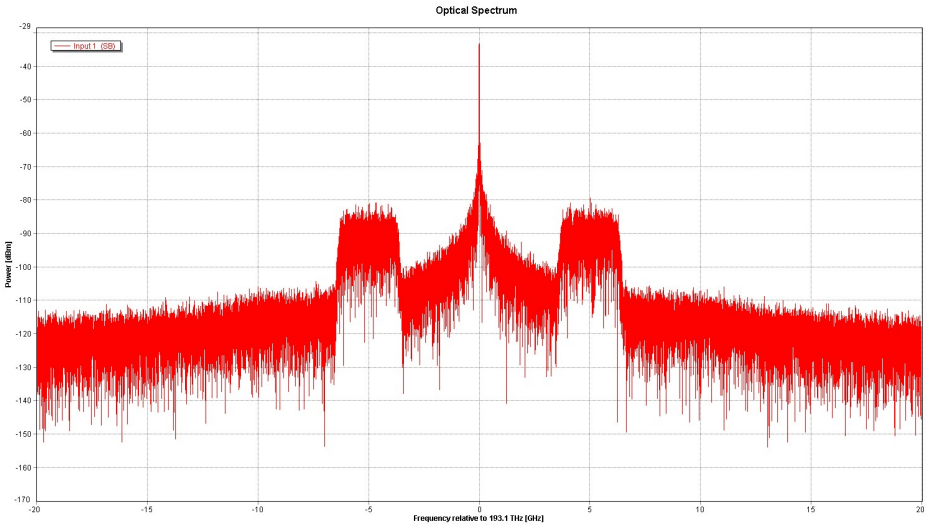

Figure 3.5: QPSK with PIN

Figure 3.5 shows that the optical OFDM signal is centered at 5GHz, and has a 2.5GBd symbol rate in order to obtain the bit rate of 10Gbit/s, because the 16-QAM modulation format have 4 bits per symbol.

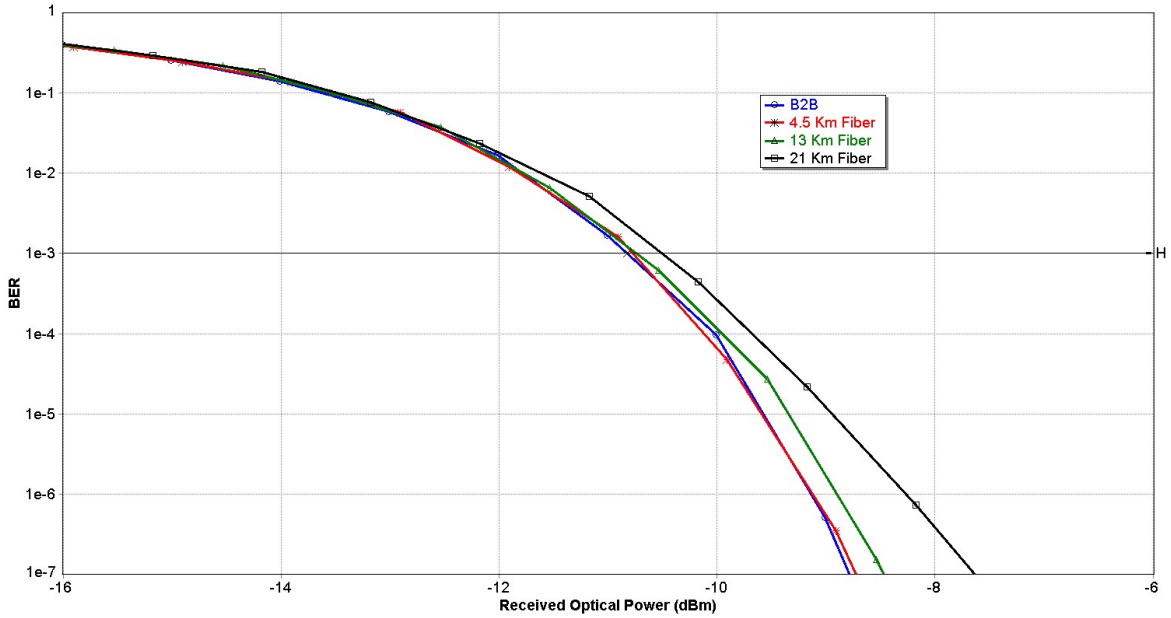

Figure 3.6: 16QAM results using a PIN

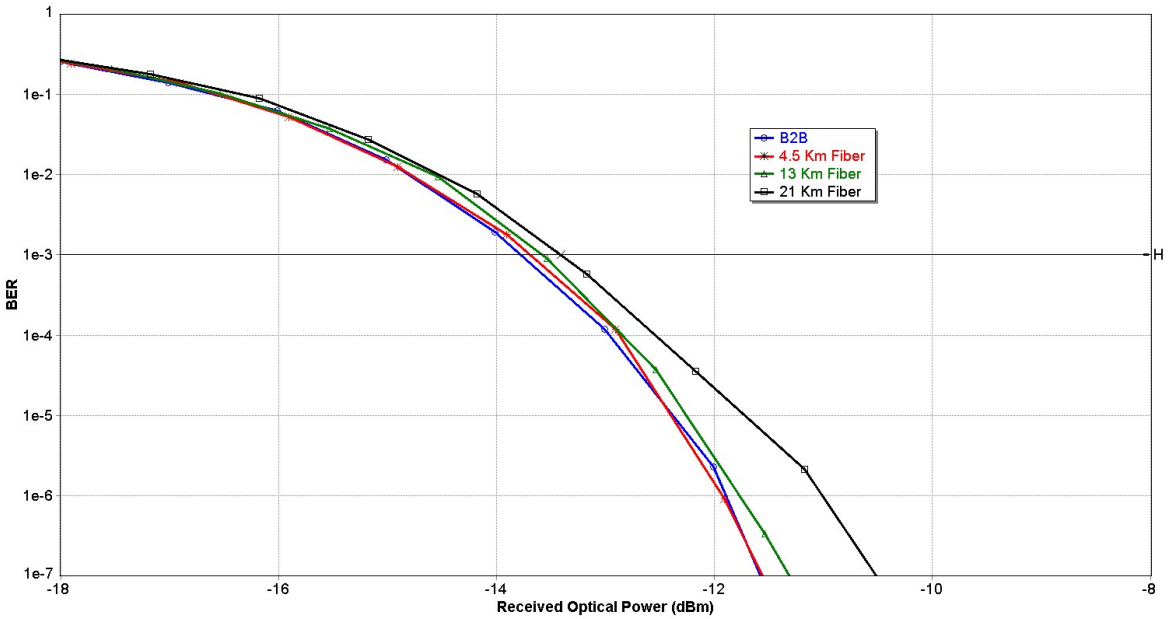

Figure 3.7: 16QAM results using a APD

In figure 3.6, it is possible to conclude that the B2B receiver sensitivity is around -10.8 dBm, and in figure 3.7, the B2B receiver sensitivity is around -13.8 dBm. These 16-QAM receiver sensitives are greater than the QPSK receiver sensitives due the symbols distance. The power penalties happen due to the chromatic dispersion, where the optical phase of the signal depends on its wavelength.

In summary, the main interest of this chapter was to study the acquired knowledge on optical OFDM in a simulation scenario. The simulation was built in order to understand each step of external modulation and direct detection behavior when using an OFDM signal. The OFDM signal was generated using two advanced modulation formats, QPSK and 16-QAM, and then it was done the comparison between them by using different detectors, a PIN and an APD.

Chapter 4

Experimental Validation

In this chapter, two external modulation setups were done in the laboratory. The first one using an MZM and the other using an RSOA, both with the same purpose, perform the E/O conversion. Before going to the complex setups, it is important to understand the characterization of each element that will be used in each setup, and understand the DSP used to generate and receive the electrical OFDM signal.

4.1 Digital Signal Processing

4.1.1 Signal Normalization

At the transmitter, the signal before being propagated it was normalized, however when the signal is received on the oscilloscope it does not appear normalized. At the figure 4.1, it is possible to observe this behavior.

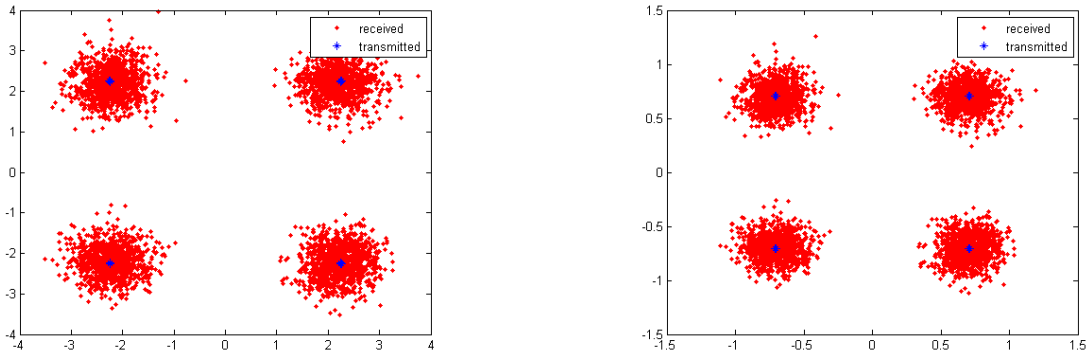

Figure 4.1: On the left, constellation without normalization. On the right, constellation with normalization.

It is required to have the received constellation decision level, equal to the decision level of the signal mapped at the transmitter, for the estimation of the BER and the error vector magnitude (EVM) to be done correctly. Thus, the signal has to be normalized again, and the equation 4.1 is used to perform it.

$$\overline{X} = \frac{signal}{\sum \sqrt{real(signal)^2 + imag(signal)^2}} \tag{4.1}$$

Where $\overline{X}$, is the signal average, that represents the distance to the axis center.

4.1.2 Phase estimation and equalization

The receiver has the capability of reporting how the signal was affected during transmission if there was a shift on amplitude, phase or both. Thus, it is needed to calculate some coefficients with correction capacity, in order to equalize and minimize distortions that emerged in the transmission. Figure 4.2 , in the left side, shows how a QPSK constellation can be corrupted, and in the right side, how a QPSK constellation can be equalized.

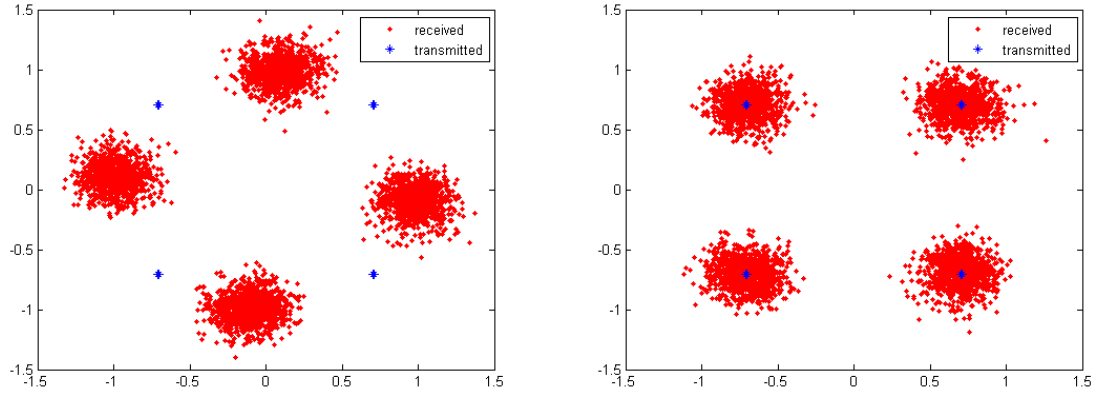

Figure 4.2: In the left side, QPSK constellation corrupted. In the right side, a QPSK constellation equalized

The rotation of the receiver information symbol constellation, can be produced by the channel chromatic dispersion or the phase noise from the transmitter or receiver lasers. The coefficient that has to be calculated with correction capacity, is the angle shift value. In the cases used here, QPSK and 16-QAM modulation formats, this angle shift value it is calculated through the equation 4.2.

$$\Theta = \frac{1}{4} * arg \cdot (\frac{1}{N} \cdot \sum_{i=0}^{N-1} signal_i^4) \tag{4.2}$$

Where N is the estimated number of samples. As the angle shift value are calculated, θ, has to be added to the normal phase shift of the QPSK and 16-QAM, that is $\frac{\pi}{4}$, as show in the equation 4.3.

$$signal = signal \times \exp^{-j(\theta + \frac{\pi}{4})} \tag{4.3}$$

The results of the equation 4.3 are shown in figure 4.2, where it is possible to observe, in the right figure, the rotation of the information symbol constellation.

This equalizer only shows a small phase shift, but probably, the constellation was rotated more than this small shift. An example of this behavior is if the combination '01' is mapped in the first quadrant at the transmitter, and at the receiver side the same combination appears in the second quadrant. The figure 4.3 shows a rotation of $\frac{3\pi}{2}$, where the blue symbols, for example, are generated at the second quadrant, and these blue symbols were received at the first quadrant.

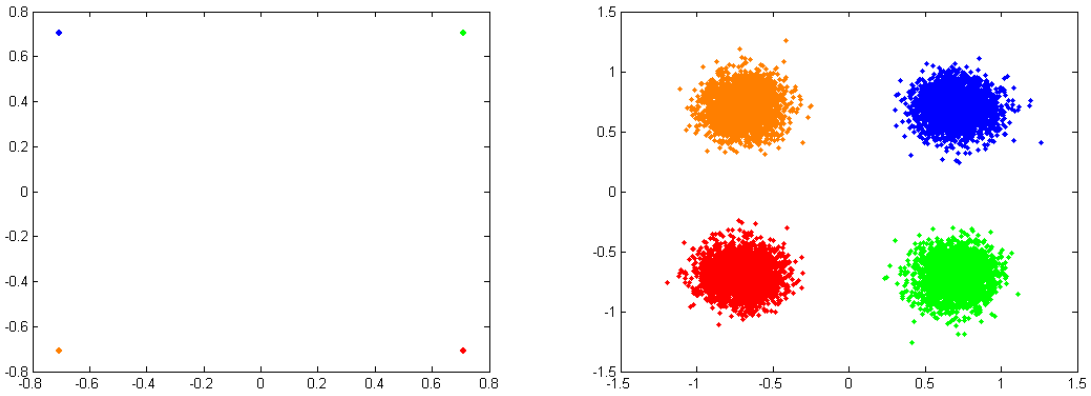

Figure 4.3: On the left side, the generated QPSK constellation. On the right side, the received QPSK constellation

The equalizer of the equation 4.3, not solve this problem, thus, the signal has to be multiplied by multiples of $\frac{\pi}{4}$, in order to obtain the best BER and EVM.

$$\theta_{rotation} = [0,\ \frac{\pi}{2},\ \pi,\ \frac{3\pi}{2}] \tag{4.4}$$

With the values of 4.4 needed to multiply the signal by all of them, as show equation 4.5.

$$Signal = Signal * \exp^{j*\theta_{rotation}} \tag{4.5}$$

With equation 4.5, it is possible to correct all the symbols distortions, and the mapped symbols will be correctly demapped at the receiver. The received constellation is now much closer to the expected.

4.1.3 Synchronization

An important step in the detection, is the symbol synchronization. As delays occur during optical transmissions, the receiver should know when it has started and finished each symbol detection window, in order to avoid information loss. Sections 4.1.1 and 4.1.2 are only possible with a correct synchronization.

There are a few ways to synchronize two signals, but in this experimental work it was used the cross-correlation. With the cross-correlation process, it is possible to know the number of bit errors that occurred during the optical transmission. The cross-correlation is a convolution of the generated signal and the received signal, where the received signal have a lag parameter. If the lag parameter is greater than one, the received signal is shifted to the right regarding the generated signal by the lag parameter value but if it is less than zero, the received signal is shifted to the left regarding the generated signal. As the arbitrary waveform generator sends the signal in real time, in each oscilloscope window appears more than one signal, thus, the cross-correlation has to be performed at the beginning, before the received signal is demodulated. The figure 4.4 shows the results of the cross-correlation between the generated and the received signal, before being demodulated.

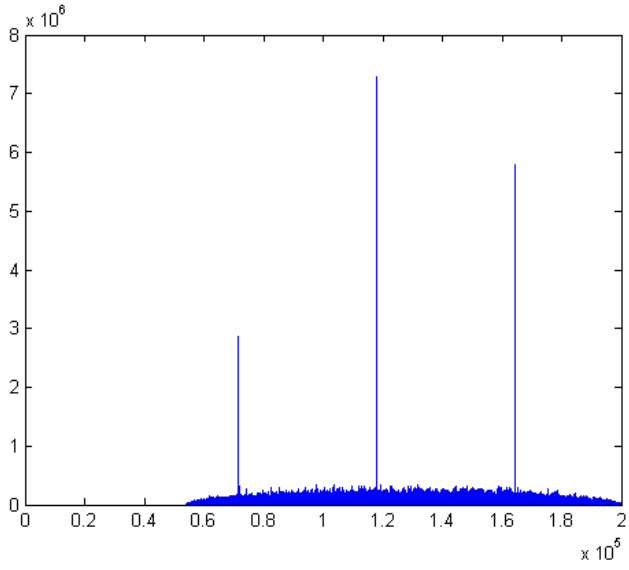

Figure 4.4: Cross-correlation before signal demodulation

Each peak of the figure 4.4, represents the position where the two signals are equal to each other.

The oscilloscope operates at 50 Gsa/s, and the QPSK and 16-QAM signals are generated with 60Gsa/s, and in order to perform the cross-correlation between them it is necessary for the detection that the generated and received signals take the same sample rate. Thus, these generated signals were interpolated by 5, resulting in a sample rate of 300 Gsa/s, and after that, a down sample by 6 was performed in order to obtain the 50 Gsa/s. As presented in section 4.4.3, the QPSK mixed with 16-QAM signal is a special case, where two signals were created with the same bit stream but with different sample rates, one with 63 Gsa/s, to be loaded into the arbitrary waveform generator, and the other with 350 Gsa/s, to be loaded in the detection in order to be compared with the received signal. But as the received signal

have a sample rate of 50 Gsa/s, will have to be interpolated by 7, in order to obtain a received sample rate of 350 Gsa/s.

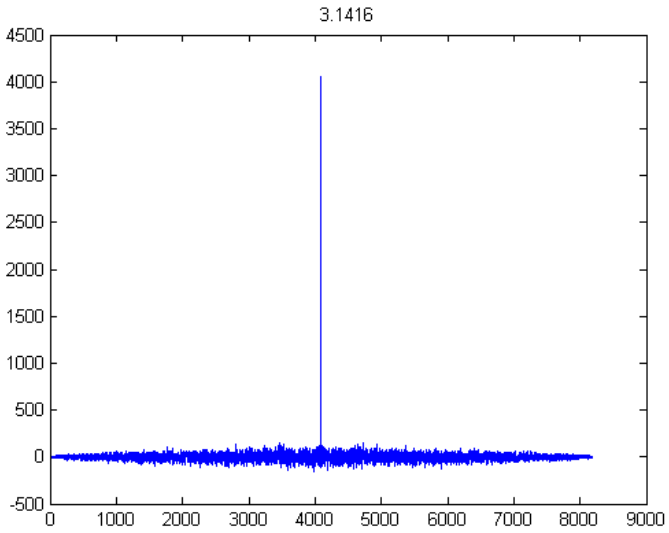

Figure 4.5: Synchronization after demodulation

After performing demodulation, cross-correlation was again used for each angle value, and the best angle found is shown in figure 4.5, where the signal samples are shown at the X axis and the correlation value is shown at the Y axis.

4.1.4 Receiver sensitivity

The receiver sensitivity is performed by the BER, the number of bit errors in a received bit stream, and by the EVM, estimating the symbol distance from the ideal location.

4.1.4.1 BER

This measurement is a key parameter, because it determines the quality of the communication channel. The BER calculation is based on the comparison of the transmitted bit stream with the received bit stream, counting the number of errors. The definition of BER can be demonstrated by the equation 4.6.

$$BER = \frac{Number\ of\ errors}{Total\ number\ of\ bits\ sent} \tag{4.6}$$

4.1.4.2 EVM

EVM is a measurement that shows the difference between the expected reference symbol and the received symbols, is another way to evaluate the quality of the communication channel. It is defined as the root mean square (RMS) value of that difference. The EVM can be demonstrated by the following equation

$$EVM = \frac{\sqrt{\frac{1}{N}\sum_{n=0}^{N-1} Ierr[n]^2 + Qerr[n]^2}}{P_0} \times 100 \quad (\%) \tag{4.7}$$

where n is the symbol index, N the number of symbols, $Ierr$ the difference between in-phase symbol reference and in-phase symbol received , $Qerr$ the difference between the quadrature symbol reference and quadrature symbol received, and P_0 is the average power of the ideal constellation. With the figure 4.6, it is possible to understand some of the parameters of the equation 4.7 [34].

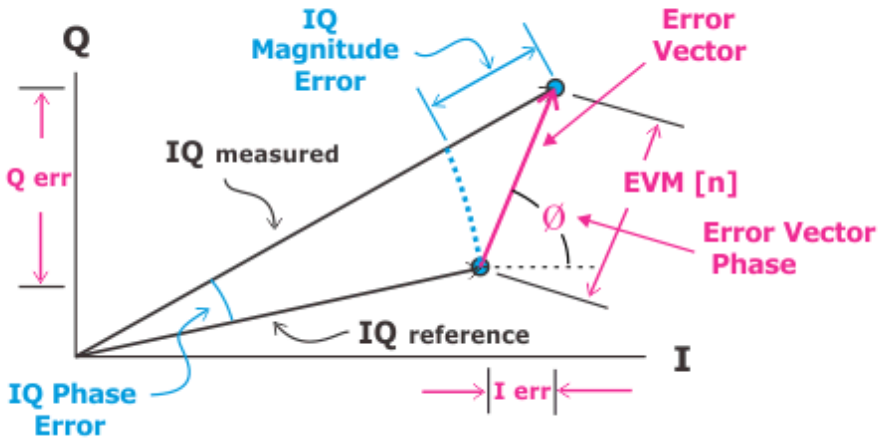

Figure 4.6: Illustration of EVM [34].

4.2 External modulators characterization

4.2.1 MZM

As present in section 2.5.1.2, the MZM linear response is in the QP. In order to obtain the experimental Quadrature point, it was prepared the setup shown in figure 4.7.

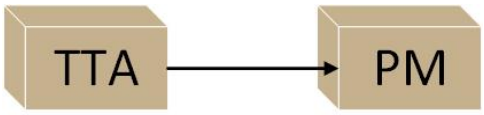

Figure 4.7: Transfer function setup

Two main blocks are used in this setup, the Tunable Transmitter Assembly (TTA) block that is composed by a 10 Gbit/s Tunable Transmitter and an MZM, and the PM. In TTA block, the bias voltage, IMB_{set}, was set to its maximum and the output power in the PM was measured in order to obtain the transfer function graph of the transmitter, as show in figure 4.8

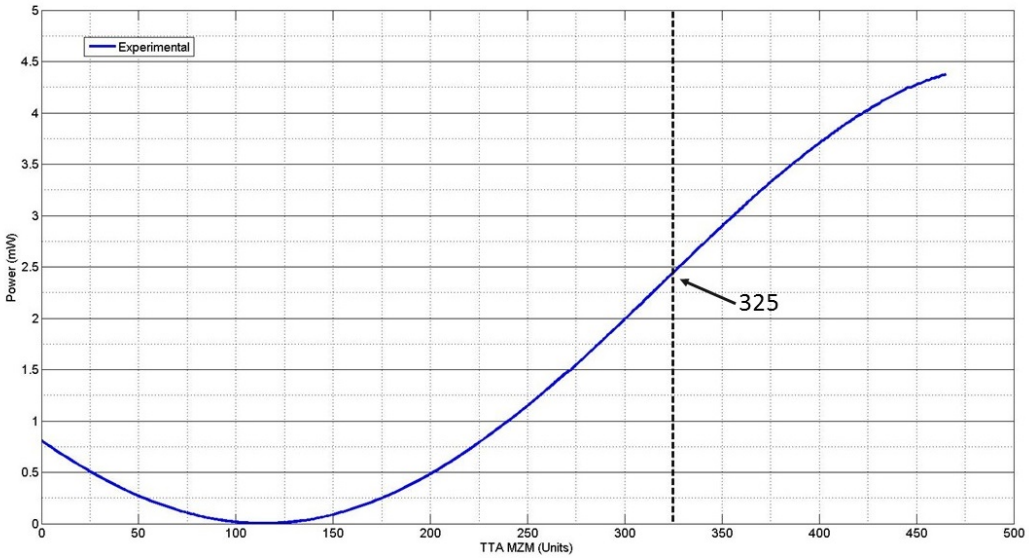

Figure 4.8: Oclaro TTA Transfer function

It is possible to see that in the x-axis the bias voltage is an absolute value, and to obtain the bias voltage in Volts, the absolute value has to be divided by 1000, as show in figure 4.9.

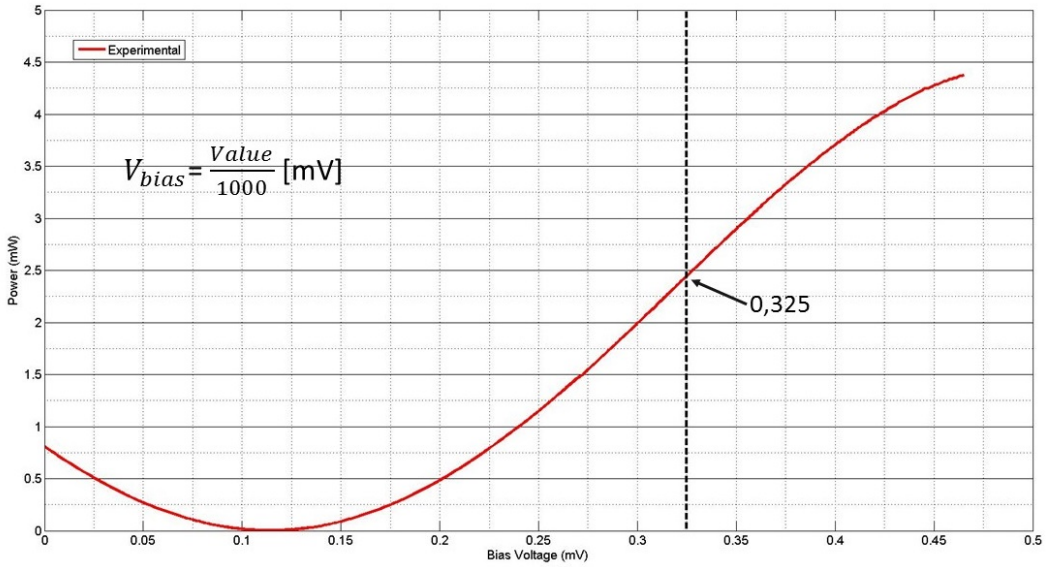

Figure 4.9: Oclaro TTA Transfer function in mV

The best bias voltage is 0.325mV, it will be proved in the setup 4.10.

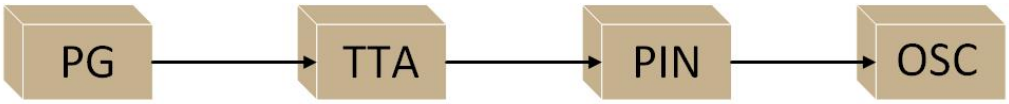

Figure 4.10: Transfer function setup with PIN

It was added to the previous setup a Pattern Generator (PG block) at 10 GHz, a PIN photodiode (PIN block) and an oscilloscope. The oscilloscope was used to measure the best extinction ratio (ER) in an eye diagram. In figure 4.11 it is possible to see that the best ER is 10.45 dB at 325 mV bias voltage.

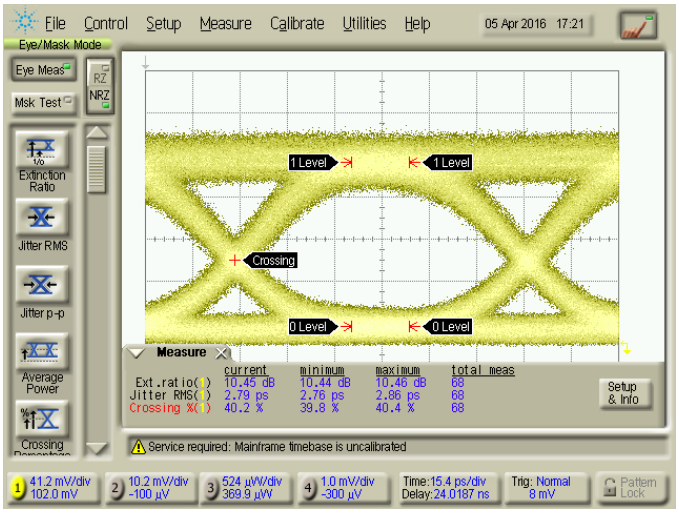

Figure 4.11: Eyw diagram at 0.325mV

4.2.2 RSOA

Before going to the RSOA setup analysis, first it is important to characterize all the devices in the setup to know their losses.

4.2.2.1 Circulator

The first device to be characterized is the circulator. The circulator has three connections. The first on the left is the input, the second on the right is the input/output and the third one is the circulator output

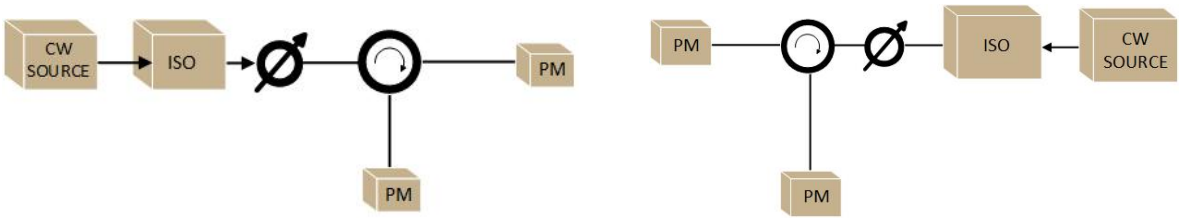

Figure 4.12: On the left, losses between circulator input and circulator input/output. On the right, losses between, circulator input/output and circulator output.

It is shown in figure 4.12 two setups to characterize the losses on both sides of the circulator. In the first setup, on the left, a setup was assembled to measure the losses between circulator input and circulator input/output, to realize that, a continuous wave source was placed on the input and two power meters in the other two connections. With the help of the attenuator, the input power was changed manually to obtain different values in both power meters. These values were subtracted to achieve the loss. The same idea was implemented in the second setup, in the right, but in this one, the continuous wave source is in the input/output in order to obtain the loss between circulator input/output and circulator output. The results obtained for the first setup was 1.52 dB and for the second setup was 1.5 dB.

4.2.2.2 Loss between input power and circulator input/output

Since the setup uses a splitter, it is crucial to measure the loss between the setup input power, upper arm of the splitter, and the circulator input/output. To perform that, was implemented the setup in the figure 4.13.

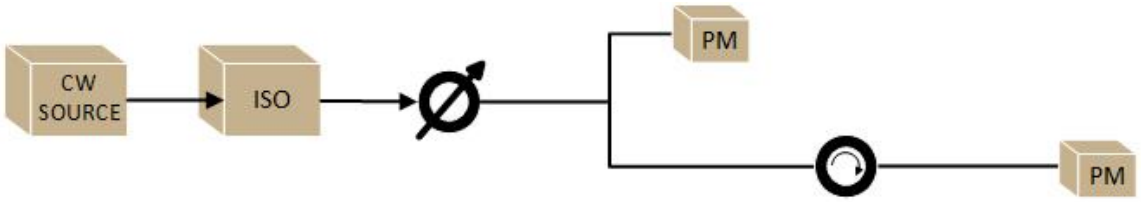

Figure 4.13: Setup to measure the loss

This setup used the same continuous wave source and attenuator which were previously used. As it is being used a splitter 80-20, 20 in the upper arm and 80 in the lower arm, it is important to know the loss from the upper arm to the circulator I/0, in order to know the RSOA input power witch is going to be used later. Thus, the input power was changed, and different values were obtained in both power meters. The average value of the loss, achieved by the power meter values subtraction, is 3.13 dB.

4.2.2.3 RSOA gain

At this moment it is possible to measure the gain. In the setup of figure 4.14 was added to the circulator I/O a RSOA, and in the circulator output was used a optical spectrum analyzer (OSA) to measure the RSOA output power.

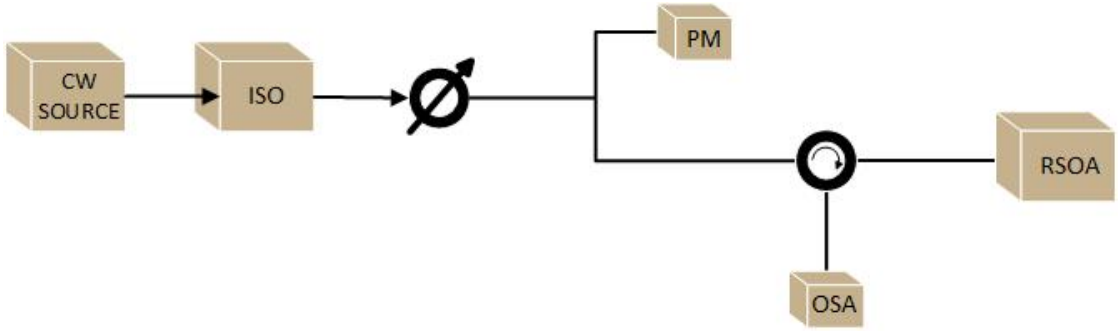

Figure 4.14: RSOA setup to measure the gain

In sections 4.2.2.1 and 4.2.2.2, it was measured the loss between the splitter upper arm and the RSOA input, and the loss between RSOA output and OSA. With these two losses, it is possible to know the RSOA input power and the RSOA output power. To a fixed input power value, it will be found one value in the power meter and another value in the OSA in dBm.

The value in the power meter must be subtracted to 3.13 dB, that was the loss from the splitter upper arm to the RSOA input, in order to obtain the RSOA input power. To measure the RSOA output power, the OSA value has to be added up to 1.5 dB, that was the loss from RSOA output and OSA. The setup input power was changed from -48 dBm until 5 dBm in 5 dB steps, and in each of these values, the RSOA bias current changed between 45 mA and 95 mA in 5 mA steps.

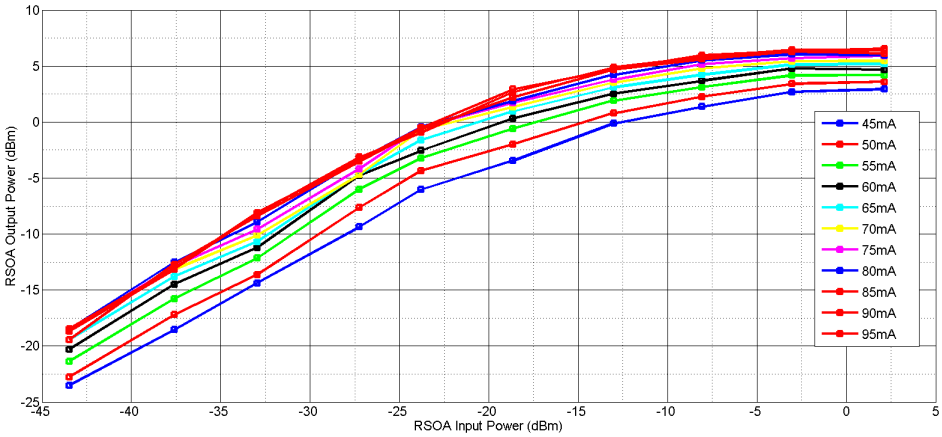

Figure 4.15: Output power VS Input Power

The figure 4.15 shows the relation of the CW optical input power with RSOA output power, and bias current plotted. It is possible to see the RSOA saturation at 5 dBm of output power. It is also possible to see that the output power increases with increasing input power, and when the bias current increases, the output power increase.

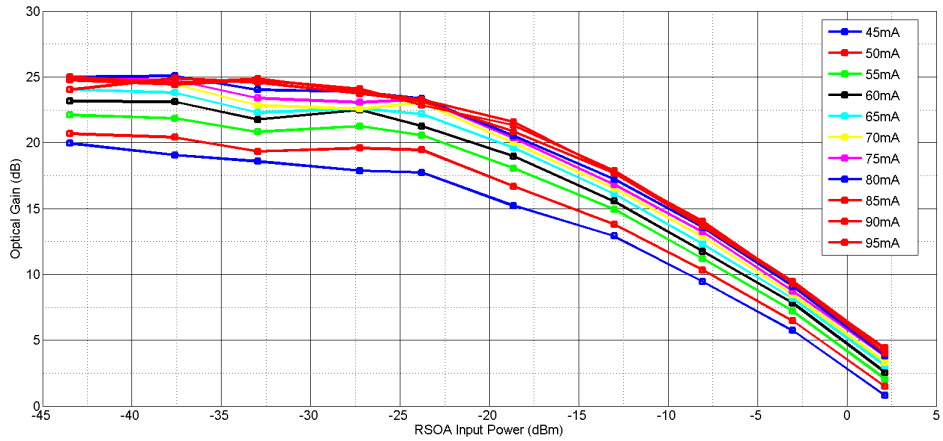

Figure 4.16: Gain VS Input power

Figure 4.16 show the RSOA optical gain versus CW optical input power, and bias current plotted. It is possible to see the RSOA saturation as the input power increase. For optical input powers of < -35 dBm, the RSOA has a larger optical gain.

The RSOA saturation is given by the equation 4.8.

$$G_{RSOA} = P_{out} - P_{in} \tag{4.8}$$

The saturation of the lower current is 20 dB, but as the current increase the gain also increases until reaching 25 dB.

4.2.3 External modulation with RSOA using NRZ

After the RSOA characterization, it is important to demonstrate the RSOA performance when using a RF signal. Regarding this, it was used a signal with less complexity than before using the OFDM signal that has more complexity. A pattern generator was used to create a pseudorandom binary sequence (PRBS) with $2^{31} - 1$ bits, that was modulated in order to obtain the non return to zero (NRZ) format. The setup that was used is shown in figure 4.17.

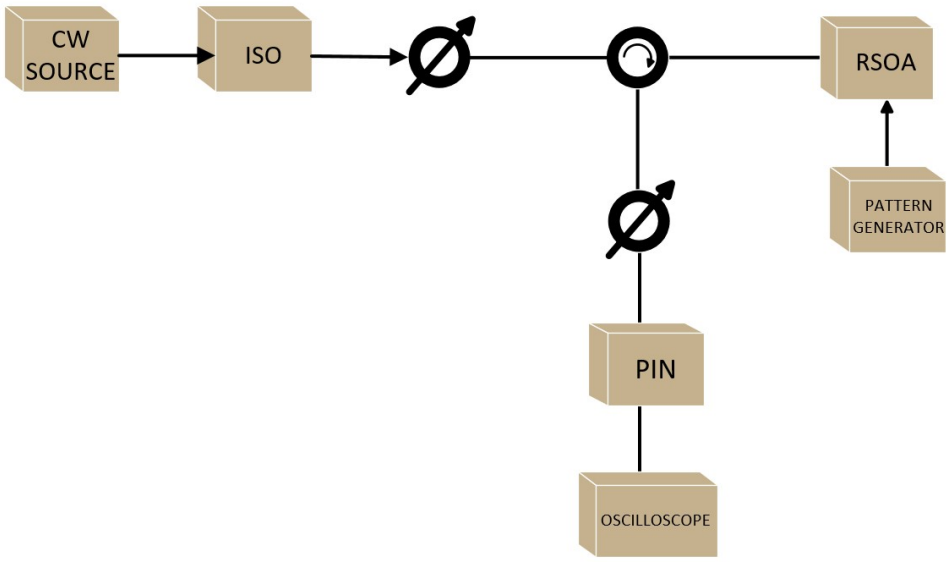

Figure 4.17: External modulation with RSOA

The electrical NRZ signal, created by the pattern generator, is combined with an optimum DC bias current to directly modulate a 1550 nm CW optical wave in the 1GHz RSOA. The output optical power from the RSOA, passes thought a Variable Optical Attenuator (VOA) to adjust the receiver optical power. A PIN was used to convert the received optical signal into the electrical domain and to perform the ER calculation. The electrical signal was inject into the oscilloscope where the ER values are shown. Figure 4.18 shows the results for a 45 mA bias current.

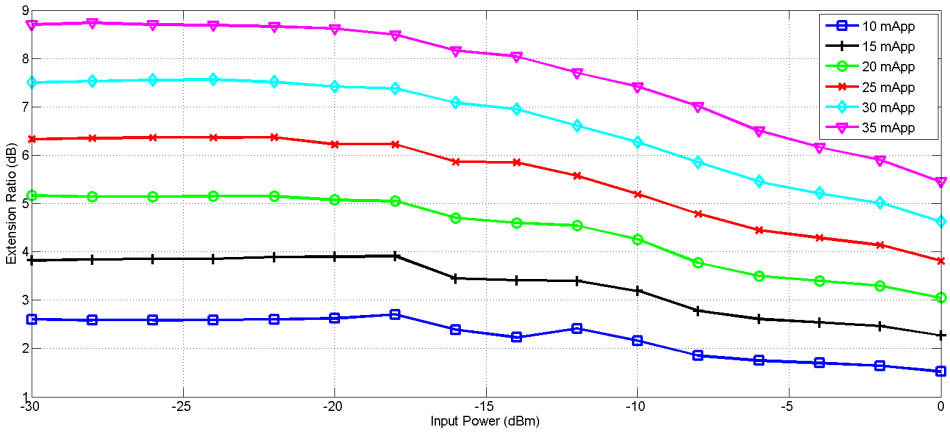

Figure 4.18: Extinction Ratio versus Input power with 45 mA bias current

Figure 4.18 shows the ER versus the setup input power for different NRZ amplitudes with fixed bias current of 45mA. Analyzing the plot, it is possible to observe that the saturation appears at lower powers and ER starts to decrease for low powers. For higher ER it is possible to obtain a better BER, that is going to be an important parameter in the section 4.4.

4.3 External modulation with RSOA using OFDM

In figure 4.17, wich has been shown above, it was shown the setup using a RF signal that was an NRZ signal generated by the pattern generator. On this section it will be shown almost the same setup but without the pattern generator because now it is going to be used other RF signal with more complexity. This signal, that was more complex, is the OFDM signal generated by off-line DSP in Matlab. Each stage of the off-line DSP of the OFDM transmitter consists of QPSK or 16-QAM symbol encoding, serial-to-parallel conversion, IFFT, CP insertion, pulse shape, up-conversion at 300 MHz and a DAC with a sampling rate of 60 Gsa/s, in order to generate the electrical OFDM signal as mentioned in the section 2.4.

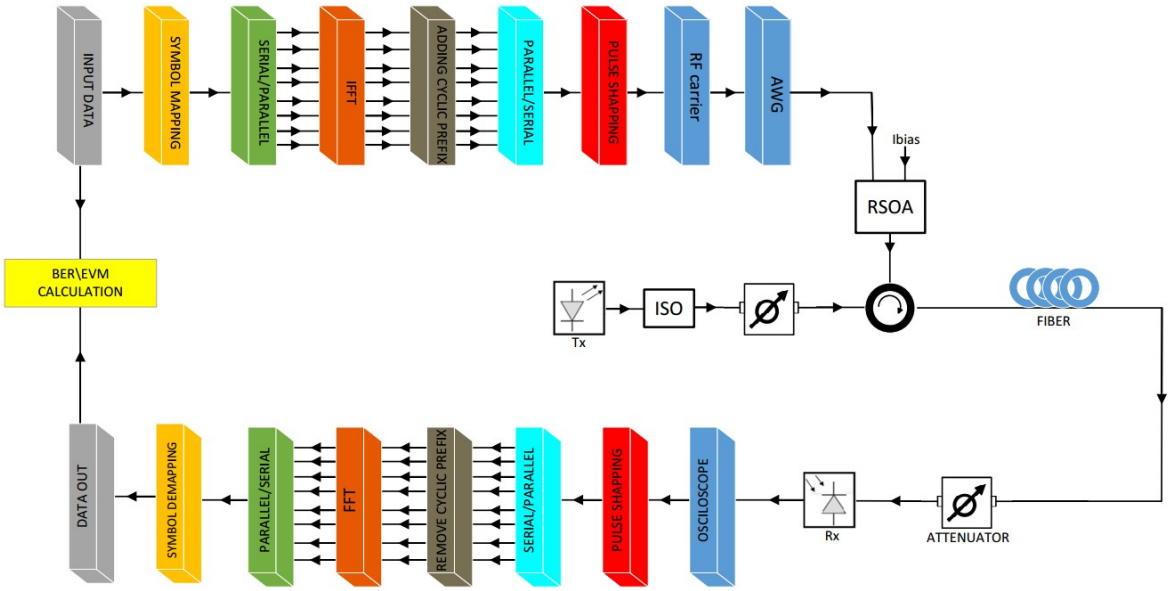

Figure 4.19: External modulation setup

The RSOA has 1 GHz bandwidth when DC-biased at 45 mA and has a small signal gain of 20 dB. Thus, it is a challenge have a bit rate of 10Gbit/s, because when it is used a symbol rate of GBd/s the RSOA, it starts to cut the signal in the borders. Regarding this problem the symbol rate was 312.5 MBd/s in order to obtain a bit rate of 625 Mbit/s when using the QPSK modulation format and 1.25 Gbit/s in case of 16-QAM modulation format. Having this two scenarios, it is known that the QPSK modulation format is more tolerant to lower values of the signal to noise ration (SNR) than the 16-QAM and due to that fact it is difficult in the receiver to recover the 16-QAM signal with a desired BER and EVM.

Figure 4.19 illustrates the experimental setup for evaluating the RSOA performance. The CW signal, produced by the tunable laser, Tx, at 1550 nm, was injected in the RSOA via a optical circulator, and an optical isolator was used to prevent any backward propagations. The RSOA input CW power from the tunable laser was fixed at -15 dBm because that is where RSOA does not have a saturated gain, as it is possible to observe in figure 4.16. A DSB electrical OFDM upstream signal generated by the arbitrary waveform generator, that converts the digital data to an analogue signal (DAC) and is combined with an optimum DC bias current to directly modulate the 1550 nm CW optical wave.

The electrical signal was then applied to the RSOA via a bias-tee. Then, the optical upstream OFDM signal passes through the optical circulator with 1.5 dB insertion loss, that is used to separate the modulated OFDM signal from the injected CW optical wave and prevent backward propagations. The output optical power from the RSOA was transmitted in different SSMF fiber lengths without optical amplification or chromatic dispersion compensation.

At the OLT receiver, VOA was used in order to adjust the received optical power. Two photodiode (Rx) types were employed, a PIN and an APD, in order to convert the received DSB OFDM signal into the electrical domain. The signal was down-converted at 300 MHz to recover the electrical signal. The received OFDM signal was captured by a real time oscilloscope at 50 GSa/s. The oscilloscope perform the ADC conversion. Thus, to recovery the data it was implemented some additional receiver off-line DSP, which include signal normalization, phase estimation and equalization, symbol synchronization, and BER/EVM calculations. All other receiver off-line DSP functions are used only to invert the way to their transmitter DSP.

OFDM DSP Parameters	***Value***	***Unit***
IFFT/FFT points per band	64	
Number of subcarriers	8	
Modulation formats	QPSK, 16-QAM	
DAC sample rate	60	GSa/s
ADC sample rate	50	GSa/s
OFDM symbol rate	312.5	MBd
Cyclic prefix	1	samples
Total samples per symbol	160	Samples
Roll-off factor	0.15	dB/decade
Carrier Frequency	300	MHz
RSOA operating conditions		
CW optical power injected	-15	dBm
Bandwith	1	GHz
Gain	20	dB
Bias current	45	mA
PIN parameters		
Detector bandwith	15	GHz
APD parameters		
Detector bandwith	22	GHz
Fiber Parameters		
Length	4.48, 13.39, 20	Km
Type	SSMF	
Loss	0.185	dB/Km

Table 4.1: Transmitter and transmission setup parameters

4.3.1 QPSK results

The electrical signal spectral generated by the arbitrary waveform generator is represented in the figure 4.20. It is possible to observe the 312.5 MHz symbol rate with a 300 MHz carrier frequency. As is known that QPSK modulation format carries 2 bits per symbol, thus it is achieved a 625 MBit/s.

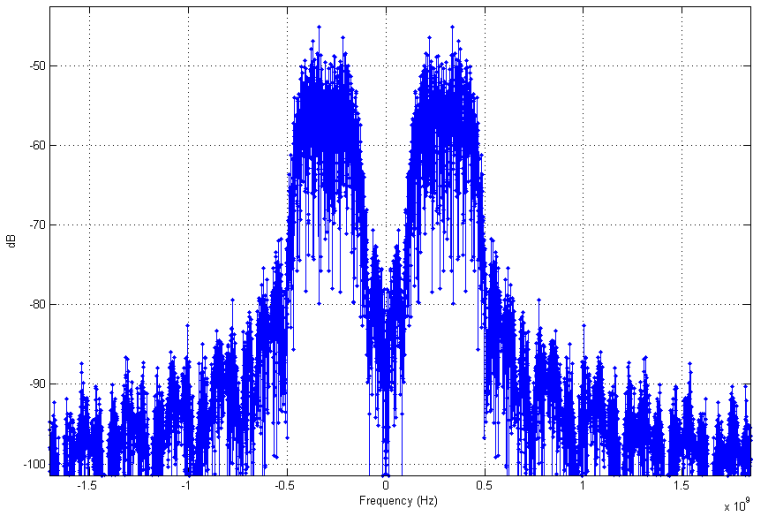

Figure 4.20: QPSK electrical spectrum

As mentioned before, in the receiver the signal passes through a VOA in order to change the received optical power and all the off-line DSP perform the BER calculations. Thus it is possible to characterize the receiver sensitivity.

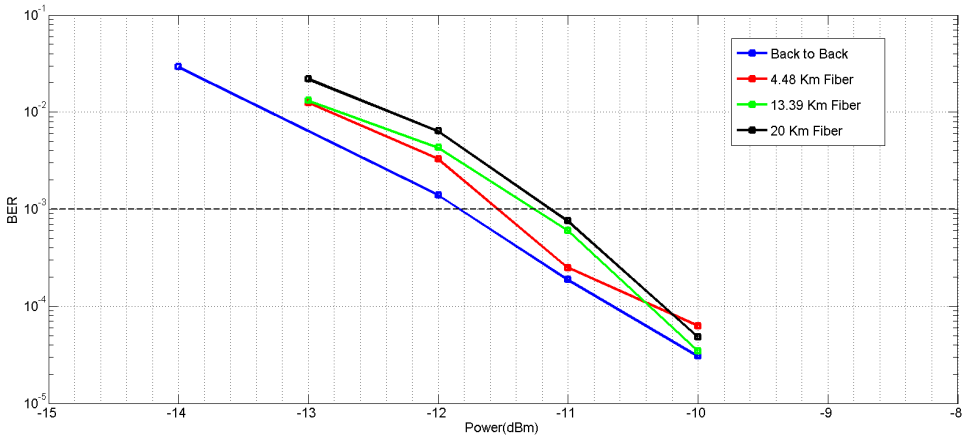

Figure 4.21: QPSK BER dependence with Received power using a PIN

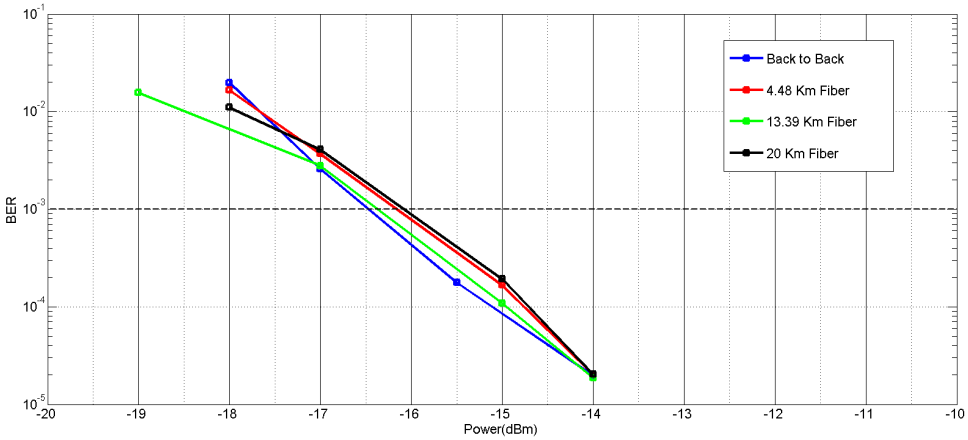

Figure 4.22: QPSK BER dependence with Received power using a APD

Figures 4.21 and 4.22 present the BER performances of RSOA using a 625 MBit/s QPSK OFDM upstream signal at the B2B, 4.48, 13.39 and 20 km SSMF.

In figure 4.21, it is possible to conclude that the receiver sensitivity it is around -12 dBm, and in figure 4.22, the receiver sensitivity is -16.5 dBm. The power penalties happen due to the chromatic dispersion, where the optical phase of the signal depends on its wavelength.

4.4 External modulation with MZM using OFDM

As already shown in the sections 2.4 and 2.5, the generation of the electrical OFDM signal, have to be done in several stages by off-line DSP in Matlab in order to transmit it through the communication channel. Each stage of the OFDM transmitter off-line DSP consists of QPSK or 16-QAM symbol encoding, serial-to-parallel conversion, IFFT, CP insertion, pulse shape, up-conversion at 5 GHz and a DAC with a sampling rate of 60 Gsa/s [35], in order to generate the electrical OFDM signal as was mentioned in the section 2.4. The setup that was used in the experimental part, is similar to the one was used in the simulation at section 3. The experimental setup is shown in figure 4.23.

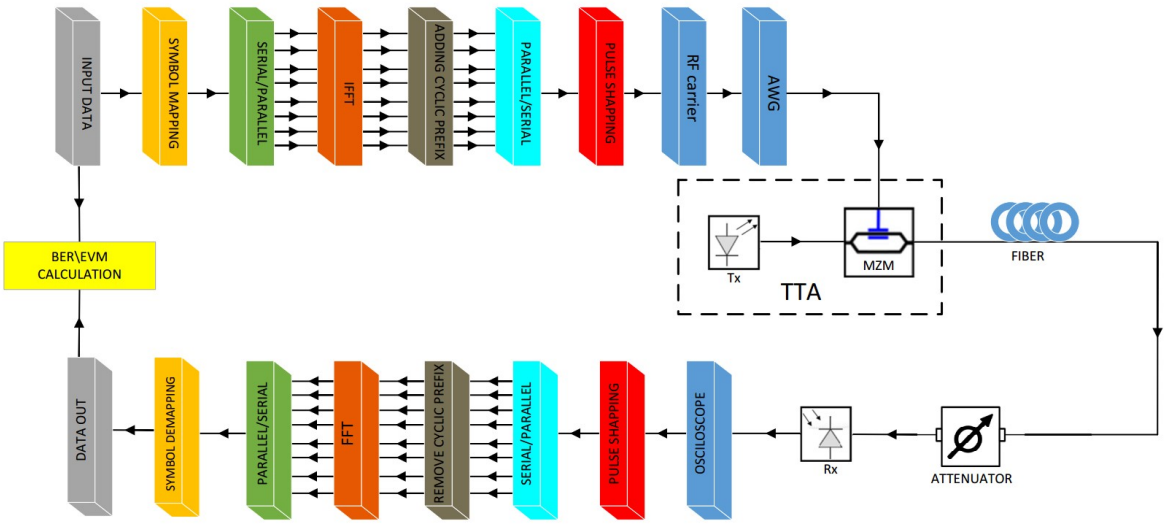

Figure 4.23: External modulation setup

In section 2.4.7 it was shown, that a DAC is needed in the transmitter and an ADC at the receiver. In this setup, the DAC is in the arbitrary waveform generator and the ADC in the oscilloscope. Thus, the first procedure, consists in loading of the OFDM signal onto the arbitrary waveform generator, that generates a analogue electrical waveform. The resulting waveform is injected into the TTA, which has been characterized in section 4.2.1, that is connected to a software in order to control the bias voltage and turn the laser on and off. In TTA, the analogue OFDM signal is combined with CW signal produced by the tunable laser (Tx) at 1550 nm. When the TTA is turned on, an optical OFDM signal is generated that can be propagated through the optical communication channel. This optical communication channel can have different SSMF lengths without optical amplification and chromatic dispersion compensation, or in the case of using a B2B topology fiber is not needed. After the fiber, it was used a VOA to change the photodiode input power in order to characterize the photodiode sensitivity. Two photodiodes (Rx) types are employed, a PIN and an APD, in order to convert the received DSB OFDM signal into the electrical domain. The signal was down-converted at 5 GHz for both modulation formats to recovery the electrical signal.

The received OFDM signal was captured by a real time oscilloscope at 50 Gsa/s, when running a Matlab script. It was possible to capture as many windows as possible to have exact results. The oscilloscope perform the ADC conversion. Each of this oscilloscope window have a size of 20^4 bits. 100 oscilloscope windows were saved on a three-dimensional vector, which was analyzed by off-line DSP. The off-line DSP in order to analyze the received signal, perform the signal normalization, the phase estimation and equalization, symbol synchronization, and BER/EVM calculations. All the received windows are compared to the generated electrical signal before injected in the arbitrary waveform generator.

OFDM DSP Parameters	***Value***	***Unit***
IFFT/FFT points per band	512	
Number of subcarriers	8	
Modulation formats	QPSK, 16-QAM	
DAC sample rate	60	GSa/s
ADC sample rate	50	GSa/s
OFDM symbol rate using QPSK	5	GBd
OFDM symbol rate using 16-QAM	2.5	GBd
Cyclic prefix	1	samples
Total samples per symbol (QPSK)	10	Samples
Total samples per symbol (16-QAM)	20	Samples
Roll-off factor	0.15	dB/decade
Carrier Frequency	5	GHz
MZM operating conditions		
Bandwith	30	GHz
Bias voltage	325	mV
PIN parameters		
Detector bandwith	15	GHz
APD parameters		
Detector bandwith	22	GHz
Fiber Parameters		
Length	4.48, 12.62, 20.82	Km
Type	SSMF	
Loss	0.185	dB/Km

Table 4.2: Transmitter and transmission setup parameters

4.4.1 QPSK modulation format

The electrical signal generated using QPSK modulation format was injected into the arbitrary waveform generator in order to obtain the electrical waveform, that is represented in the figure 4.24. As the QPSK modulation format have 2 bits per symbol and the symbol rate is 5 GBd, the electrical signal has a bit rate of 10 Gbit/s, and a sample rate of 60 Gsa/s .

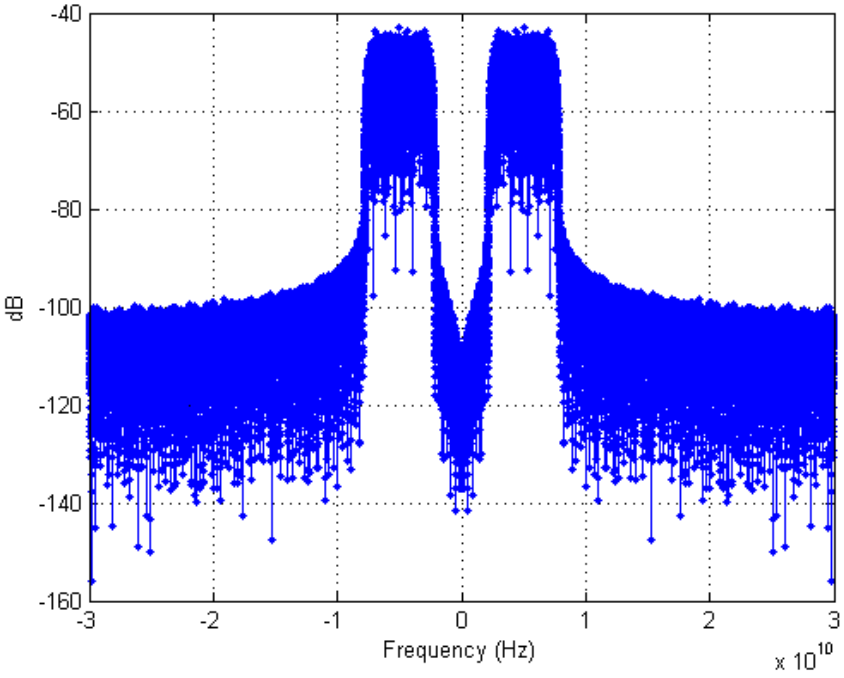

Figure 4.24: QPSK spectrum signal

As mentioned before, at the receiver the signal passes through a VOA in order to change the received optical power and all the off-line DSP perform the BER calculations. Thus it is possible to characterize the receiver sensitivity.

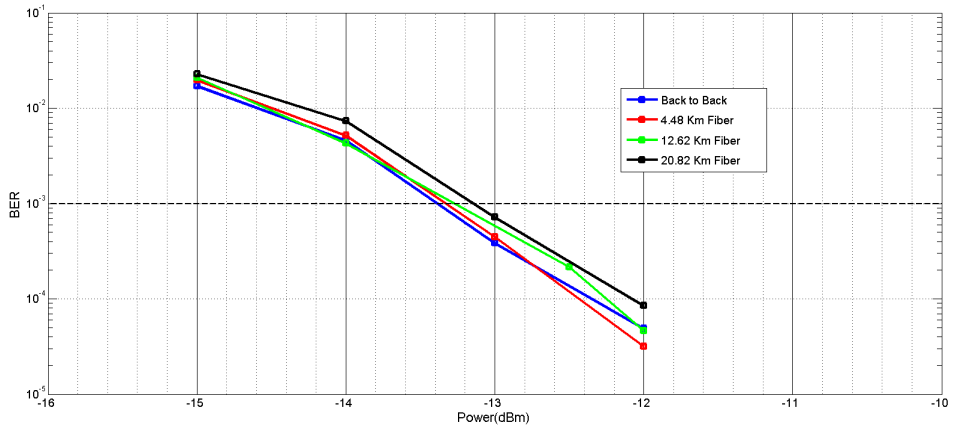

Figure 4.25: QPSK BER dependence with Received power using a PIN

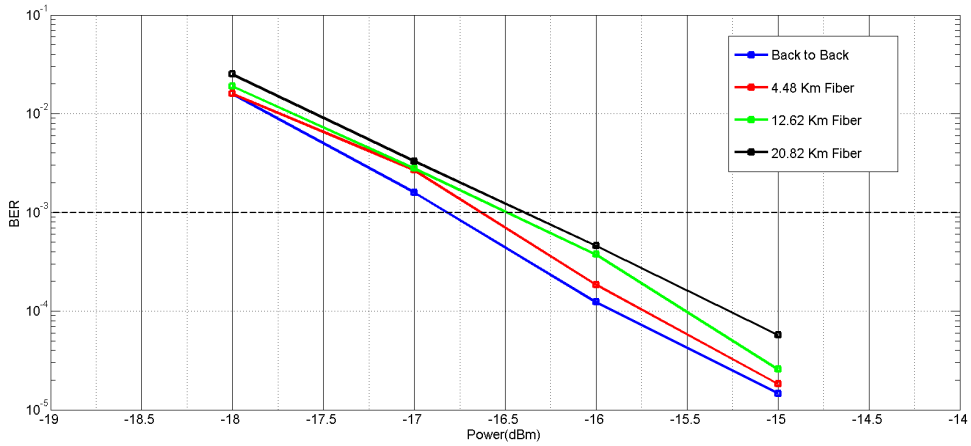

Figure 4.26: QPSK BER dependence with Received power using a APD

Figures 4.25 and 4.26 presents BER performances using a 10 GBit/s QPSK OFDM upstream signal at the B2B, 4.48, 12.62 ans 20.82 km SSMF.

In figure 4.25, it is possible to conclude that the B2B receiver sensitivity is around -13.4 dBm, and in figure 4.26, the B2B receiver sensitivity is around -16.8 dBm. The power penalties happen due to the chromatic dispersion, where the optical phase of the signal depends on its wavelength.

4.4.2 16-QAM modulation format

The electrical signal created by using a 16-QAM modulation format, was loaded into the arbitrary waveform generator. As the 16-QAM modulation format have 4 bits per symbol and the symbol rate is 2.5 GBd, the electrical signal has a bit rate of 10 Gbit/s. The figure 4.27 shows the 16-QAM spectrum signal, and a sample rate of 60 Gsa/s .

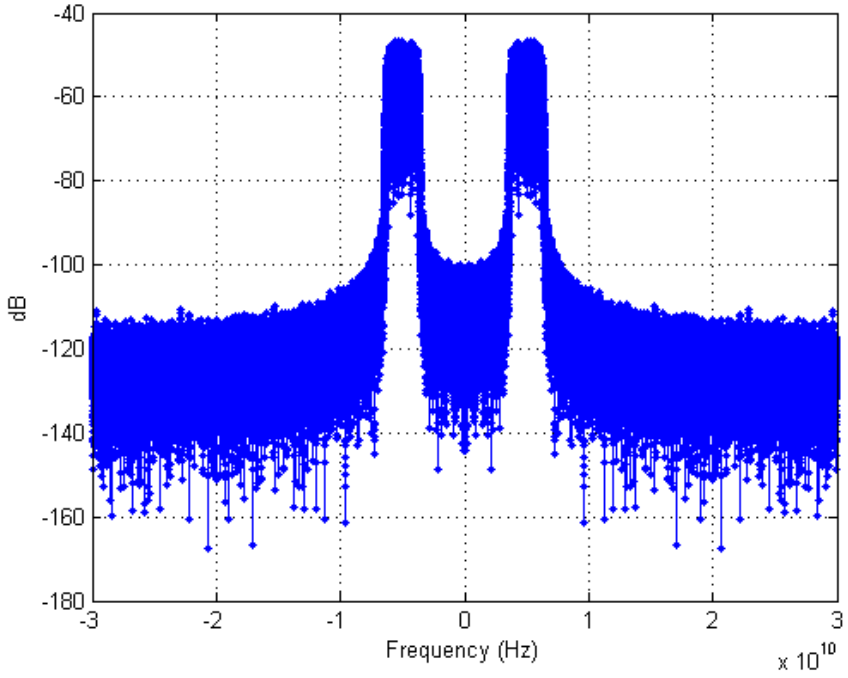

Figure 4.27: 16-QAM spectrum signal

It is shown in the figures below, the BER performance in different received powers. Thus it is possible to characterize the receiver sensitivity.

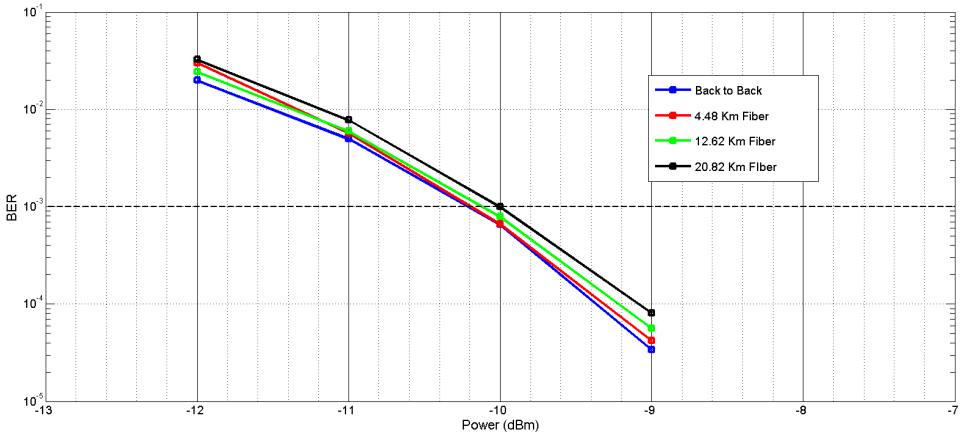

Figure 4.28: 16-QAM BER dependence with Received power using a PIN

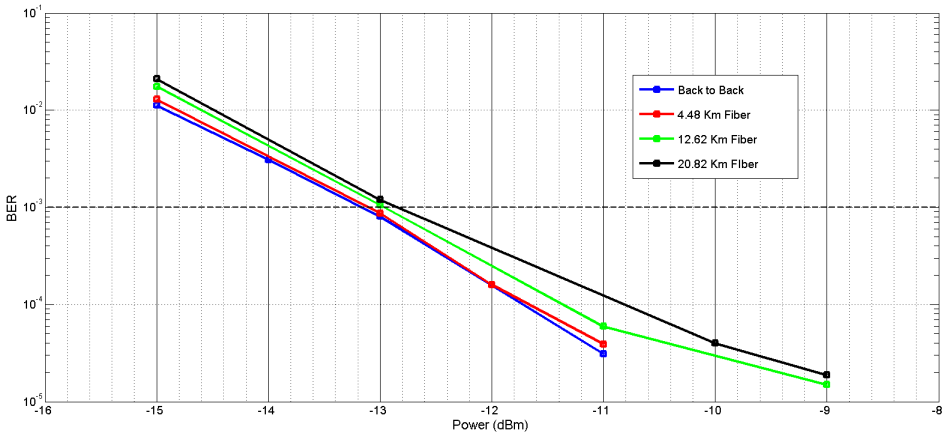

Figure 4.29: 16-QAM BER dependence with Received power using a APD

Figures 4.28 and 4.29 presents BER performances using a 10 GBit/s 16-QAM OFDM upstream signal at the B2B, 4.48, 12.62 ans 20.82 km SSMF.

In figure 4.28, it is possible to conclude that the B2B receiver sensitivity is around -10.2, and in figure 4.29, the B2B receiver sensitivity is around -13.1. The power penalties happen due to the chromatic dispersion, where the optical phase of the signal depends on its wavelength.

4.4.3 QPSK mixed with 16-QAM modulation format

On the previous experiments, all the subcarriers were using the same modulation format, but in this case both modulations formats are used. It was used QPSK modulation in the borders and 16-QAM modulation in the middle subcarriers, because QPSK deals better with bandwidth distortion due to the distance of symbols. As spoken in section 4.1, it is a challenge have a bit rate of 10 Gbit/s by using standard symbol rates, for example, 2.5 GBd, 3.125 GBd or 5 GBd.

$$BitRate = \frac{SymbolRate * 2 + SymbolRate * 4}{2} \quad Gbit/s \tag{4.9}$$

The bit rate is given by the equation 4.9, where the symbol rate is 3.5 GBd. Replacing the symbol rate at the equation 4.9, it is obtained a bit rate of 10.5 Gbit/s.

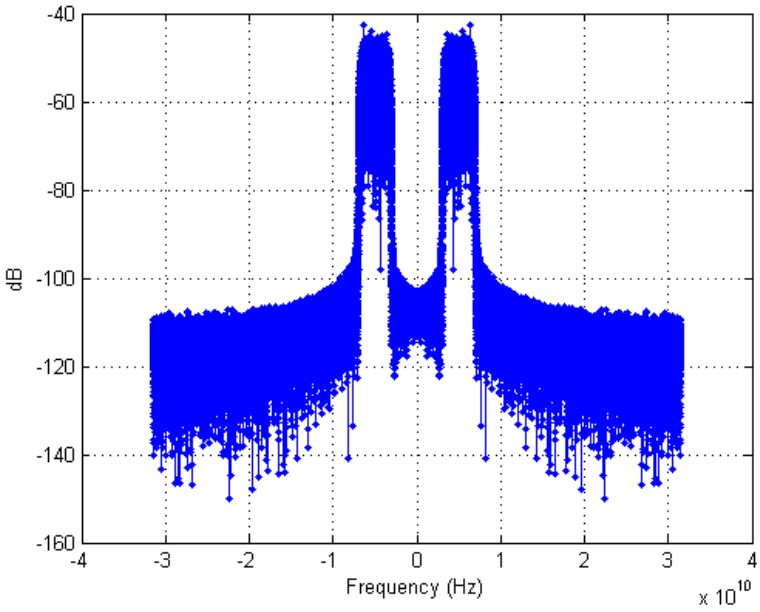

Figure 4.30: QPSK mixed with 16-QAM spectrum signal

The arbitrary waveform generator has some limitations, one of them is the sample rate, which only operates at samples rates between 55 Gsa/s and 64 Gsa/s. Due this, two signals were created with the same bit stream one with 63 Gsa/s, shown at figure 4.30, and other with 350 Gsa/s. The first one was created to load into the arbitrary waveform generator, while the second was created to help in the signal synchronization at the receiver. The figures below show the results for mixed subcarriers for multiple fiber lengths.

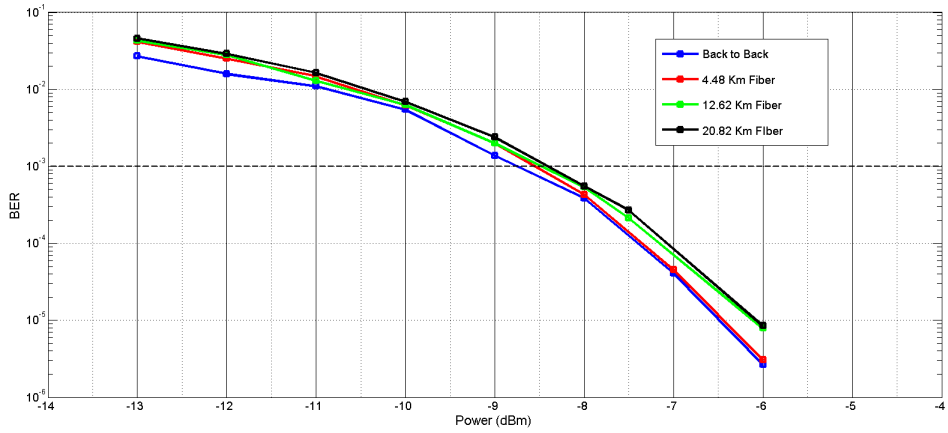

Figure 4.31: QPSK mixed with 16-QAM BER dependence with Received power using a PIN

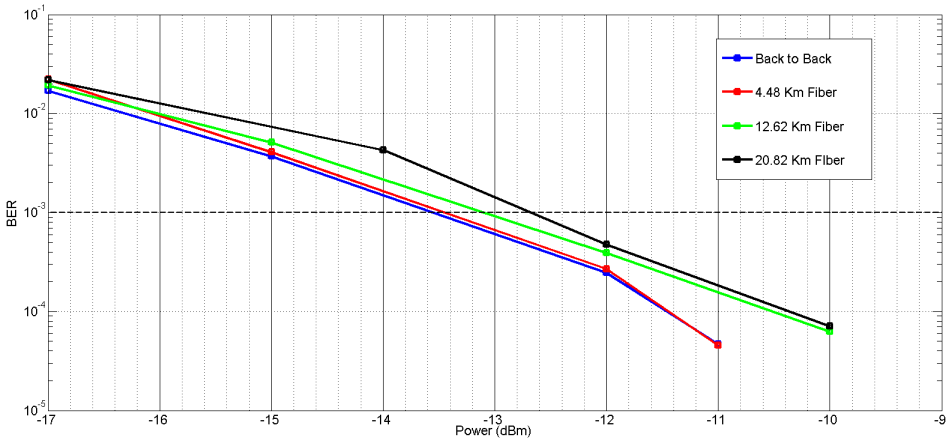

Figure 4.32: QPSK mixed with 16-QAM BER dependence with Received power using a APD

Figures 4.31 and 4.32 presents BER performances using a 10 GBit/s QPSK mixed with 16-QAM OFDM upstream signal at the B2B, 4.48, 12.62 ans 20.82 km SSMF.

In figure 4.31, it is possible to conclude that the B2B receiver sensitivity is around -8.7, and in figure 4.32, the B2B receiver sensitivity is around -13.6. The power penalties happen due to the chromatic dispersion, where the optical phase of the signal depends on its wavelength.

This chapter had as main objective the validation of the results that were obtained through simulation.

Chapter 5

Conclusions and Future Work

5.1 Conclusions

The exponentially growing demand for bandwidth arises a strong need of upgrading the existing access networks. In this master thesis, OFDM-PON was proposed and demonstrated to be also an advantageous technology for future broadband optical access networks. OFDM has been a popular technology with important applications for digital communications.

This master thesis starts with an introduction to OFDM concept and its main advantages. An extensive theoretical and mathematical study was performed in order to understand all the main aspects concerning the use of OFDM in optical transmissions.

In chapter 3 software VPI Transmission Maker was used to perform the external modulation scenario involving the MZM as external modulator. Two modulation formats were tested, QPSK and 16-QAM. Also two receivers were used, a PIN and an APD. It is possible to conclude that the receiver sensitivity decreases for longer optical fiber lengths and for high optical input powers. The power penalties between different fiber lengths is due the fiber dispersion, because the power penalties disappear when the dispersion parameter is set to zero. Also, it is concluded that the APD receiver has better sensitivity than the PIN in both modulation formats because the APD have an internal gain. The simulation using the RSOA as external modulator could not be performed due to some problems in VPI.

In chapter 4, two external modulation architectures were performed, one with an MZM and the other using an RSOA with the goal of applying to the upstream colorless links. The results of the RSOA shows that with the setup used in this work, the RSOA are not capable to achieve the data rate of 10 Gbit/s, because the RSOA has bandwidth limitations. It is a challenge having a data rate of 10 Gbit/s, because when it is used a symbol rate of Gbd the RSOA, it starts to cut the signal in the borders. In the RSOA setup, it was only used the QPSK modulation format because it is more tolerant to lower values of the SNR than the 16-QAM, and due to the fact that it is difficult to recover the 16-QAM signal in the receiver with a desired BER. The results of the MZM, working on QP, shows that if all the subcarriers use the same modulation format, the system is capable to perform at a data rate of 10 Gbit/s for distances in the order of tens of kilometers. But, if used both modulation formats (QPSK mixed with 16-QAM) to create the OFDM signal, it is a challenge have a bit rate of 10 Gbit/s by using standard symbol rates. To perform the correct demodulation all the mathematical study helped in this chapter, in order to establish the synchronization between the generated and the received OFDM signal and minimize the distortions that emerged in the transmission.

In both chapters, 3 and 4, results were obtained using a PIN and an APD, where it is possible to conclude that the APD has the best sensitivity. Two modulations formats were used, QPSK, the one who gives the best performance in the received optical power, and 16-QAM that is less tolerant to the noise.

The results of chapter 3 are in accordance with the results of chapter 4.

5.2 Future work

All the experimental and simulation work reported were focused on achieving 10 Gbit/s upstream traffic, using external modulation and direct detection. With the increase in network requirements and capacities, other OFDM variants can be performed in order to improve the transmission performance. Regarding this, it is suggested as future work the following topics:

- Analyse different number of subcarriers towards the network flexibility in terms of data rate.
- Theoretical and experimental analysis of OFDM-PON using coherent detection is a challenging work.
- A theoretical and experimental bit rate improvement up to 10 Gbit/s upstream traffic in a SSMF, using a commercially available RSOA.
- All the work reported so far have been using off-line DSP, thus, it is proposed the use of real-time DSP with the support of a Field-programmable gate array (FPGA).

Bibliography

[1] William Shieh and Ivan Djordjevic. *Orthogonal Frequency Division Multiplexing for optical communication*. Academic Press, Waltham, 2010.

[2] A. Shapari, R. M. Ferreira, R. S. Luís, Z. Vujicic, F. P. Guiomar, J. D. Reis, and A. L. Teixeira. Coherent access: a review [Invited paper]. *IEEE/OSA Journal of Lightwave Tech., in Press, DOI 10.1109/JLT.2016.2623793*, 2016.

[3] A. Shahpari, J. D. Reis, R. Ferreira, M. Lima D. Neves, and A. Teixeira. Terabit+ (192× 10 Gb/s) Nyquist shaped UDWDM coherent PON with upstream and downstream over a 12.8 nm band. *Journal of Lightwave Technology*, 32(4):729–735, 2014.

[4] Nirwan Ansari and Jingjing Zhang. *Media Access Control and Resource Allocation: For Next Generation Passive Optical Networks*. Springer Science & Business Media, 2013.

[5] Leonid G Kazovsky, Ning Cheng, Wei-Tao Shaw, David Gutierrez, and Shing-Wa Wong. *Broadband Optical Access Networks*. John Wiley & Sons, 2011.

[6] Ryohei Urata, Cedric Lam, Hong Liu, and Chris Johnson. High performance, low cost, colorless ONU for WDM-PON. In *National Fiber Optic Engineers Conference*, pages NTh3E–4. Optical Society of America, 2012.

[7] Yuanqiu Luo, Xiaoping Zhou, Frank Effenberger, Xuejin Yan, Guikai Peng, Yinbo Qian, and Yiran Ma. Time-and Wavelength-Division Multiplexed Passive Optical Network (TWDM-PON) for next-generation PON stage 2 (NG-PON2). *Journal of Lightwave Technology*, 31(4):587–593, 2013.

[8] Altice Labs. Evolution of FTTH Networks for NG-PON2. *Altice Labs WHITE PAPER*, 2013.

[9] Neda Cvijetic, Dayou Qian, Junqiang Hu, and Ting Wang. Orthogonal Frequency Division Multiple Access PON (OFDMA-PON) for colorless upstream transmission beyond 10 gb/s. *IEEE Journal on Selected Areas in Communications*, 28(6):781–790, 2010.

[10] Kun Qiu, Xinwen Yi, Jing Zhang, Hongbo Zhang, Mingliang Deng, and Chongfu Zhang. OFDM-PON optical fiber access technologies. In *Communications and Photonics Conference and Exhibition, 2011. ACP. Asia*, pages 1–9. IEEE, 2011.

[11] Charan Langton. Intuitive Guide to Principles of Communications: Orthogonal Frequency Division Multiplex (OFDM) Tutorial, 2004.

[12] Louis Litwin and Michael Pugel. The principles of OFDM. *RF signal processing*, 2:30–48, 2001.

[13] National Instruments. OFDM and Multi-Channel Communication Systems. *OPEN DOCUMENT*, Nov 2014.

[14] Fred Buchali, Roman Dischler, and Xiang Liu. Optical OFDM: A promising high-speed optical transport technology. *Bell Labs Technical Journal*, 14(1):125–146, 2009.

[15] Jean Armstrong. OFDM for Optical Communications. *Journal of lightwave technology*, 27(3):189–204, 2009.

[16] Peng Tan and Norman C Beaulieu. Reduced ICI in OFDM systems using the better than raised-cosine pulse. *IEEE Communications Letters*, 8(3):135–137, 2004.

[17] Pei Xiao, Ciaran Toal, Dwayne Burns, Vicent Fusco, and Colin Cowan. Transmit and receive filter design for OFDM based WLAN systems. In *Wireless Communications and Signal Processing (WCSP), 2010 International Conference on*, pages 1–4. IEEE, 2010.

[18] Masoud Salehi John G. Proakis. *Digital Communications*, volume 5. Fifth Edition The McGraw-Hill Companies, 2008.

[19] National Instruments. LO Phase Shift for IQ Modulator-Demodulator. `https://awrcorp.com/download/faq/english/questions/lo_iq_mod_dmod.aspx`. Accessed: 2016-10-18.

[20] Gary Breed. A tutorial introduction to optical modulation techniques. *High frequency design optical modulation, From May*, 2007.

[21] Milorad Cvijetic. *Optical Transmission Systems Engineering*. Artech House, 2004.

[22] Moustafa H Nazmi A. Mohammed, Yasmine El-Guindy. System Optimization to Eliminate Chirping in Dual Drive LiNbO3 MZM at 40 Gb/s. *International Journal of Advanced Engineering Research and Science (IJAERS)*, 1, July 2014.

[23] JMB Oliveira, HM Salgado, and MRD Rodrigues. Large Signal Analysis of Mach-Zehnder Modulator Intensity Response in a Linear Dispersive Fiber. 2005.

[24] Preetpaul S Devgan, Dean P Brown, and Robert L Nelson. RF Performance of Single Sideband Modulation Versus Dual Sideband Modulation in a Photonic Link. *Journal of Lightwave Technology*, 33(9):1888–1895, 2015.

[25] Craig Michie, AE Kelly, and Ivan Andonovic. Reflective Semiconductor Optical Amplifiers for passive optical networks. In *2009 11th International Conference on Transparent Optical Networks*, pages 1–4. IEEE, 2009.

[26] Zoran Vujičić, Rogerio P Dionísio, Ali Shahpari, Natasa B Pavlović, and Antonio Teixeira. Efficient dynamic modeling of the reflective semiconductor optical amplifier. *IEEE Journal of Selected Topics in Quantum Electronics*, 19(5):1–10, 2013.

[27] BY Cao, ML Deng, QW Zhang, RP Giddings, M Wang, and JM Tang. RSOA Intensity Modulator Frequency Chirp-Enhanced Optical OFDM PON Performance. *IEEE Photonics Journal*, 7(3):1–11, 2015.

[28] JL Wei, A Hamié, RP Gidding, E Hugues-Salas, X Zheng, S Mansoor, and JM Tang. Adaptively modulated optical OFDM modems utilizing RSOAs as intensity modulators in IMDD SMF transmission systems. *Optics express*, 18(8):8556–8573, 2010.

[29] Ezra Ip, Alan Pak Tao Lau, Daniel JF Barros, and Joseph M Kahn. Coherent Detection in Optical Fiber Systems. *Optics express*, 16(2):753–791, 2008.

[30] Joseph George K.N. Asha R.S. Veneetha Nair. Performance analysis of direct detection and coherent detection system for optical OFDM using QAM and DPSK. *IOSR Journal of Engineering (IOSRJEN)*, 3(7):24–29, 2013.

[31] John M Senior and M Yousif Jamro. *Optical Fiber Communications: principles and practice*. Pearson Education, 2009.

[32] Govind P.Agrawal. *Fiber-Optic Communication Systems*. The Institute of Optics University of Rochester , NY, 2002.

[33] Harry JR Dutton. *Understanding Optical Communications*. Prentice Hall PTR New Jersey, 1998.

[34] Keysight Technolgies. EVM (Digital Demod). `http://rfmw.em.keysight.com/wireless/helpfiles/89600B/WebHelp/Subsystems/digdemod/content/digdemod_symtblerrdata_evm.htm`. Accessed: 2016-11-03.

[35] Reginaldo B Nunes, Ali Shahpari, Jair AL Silva, Mario Lima, Paulo SB de André, and Marcelo EV Segatto. Experimental Demonstration of a 33.5-Gb/s OFDM-Based PON With Subcarrier Pre-Emphasis. *IEEE Photonics Technology Letters*, 28(8):860–863, 2016.